ACS NANO

www.acsnano.org

PERSPECTIVE

Nanomaterial-Based Artificial Vision Systems: From Bioinspired Electronic Eyes to In-Sensor Processing Devices

Changsoon Choi,[¶] Gil Ju Lee,[¶] Sehui Chang,[¶] Young Min Song,[*] and Dae-Hyeong Kim[*]

Cite This: https://doi.org/10.1021/acsnano.3c10181

ABSTRACT: High-performance robotic vision empowers mobile and humanoid robots to detect and identify their surrounding objects efficiently, which enables them to cooperate with humans and assist human activities. For error-free execution of these robots' tasks, efficient imaging and data processing capabilities are essential, even under diverse and complex environments. However, conventional technologies fall short of meeting the high-standard requirements of robotic vision under such circumstances. Here, we discuss recent progress in artificial vision systems with high-performance imaging and data processing capabilities enabled by distinctive electrical, optical, and mechanical characteristics of nanomaterials surpassing the limitations of traditional silicon technologies. In particular, we focus on nanomaterial-based electronic eyes and in-sensor processing devices inspired by biological eyes and animal visual recognition systems, respectively. We provide perspectives on key nanomaterials, device components, and their functionalities, as well as explain the remaining challenges and future prospects of the artificial vision systems.

KEYWORDS: *nanomaterial, soft electronics, robotic vision, bioinspired electronic eye, in-sensor processing*

INTRODUCTION

Advanced mobile and human-friendly robots, such as unmanned aerial systems, autonomous vehicles, and humanoid robots, have shown great potential to change human lifestyles and bring enormous benefits to society (Figure 1a).[1] These robots autonomously navigate dynamic and complex situations, operate within hazardous and unstructured environments, and perform requested roles without human intervention or even replace humans in various scenarios.[2,3] A critical enabler for such capabilities is their ability to perceive, interpret, and interact with their surroundings by collecting and analyzing a vast amount of visual data.[4,5] The visual data, which include key attributes of nearby objects such as identity, location, motion, and shape, form a solid foundation for establishing the digital-twin system.[6−8] Hence, advanced robotics necessarily leads to an increasing demand for advanced artificial vision systems that even outperform the human vision system.[9,10]

The key performance requirements of the robotic vision include accurate detection and efficient identification of target objects.[11,12] If diverse imaging situations under various environments are considered, there is a pressing need for application-specific imaging capabilities of robotic vision. For example, to ensure comprehensive observation of the entire region-of-interest without blind spots, it is important to achieve panoramic imaging capability allowing clear capture of all objects located across wide ranges of field-of-views (FoVs) and distances (Figure 1b).[13,14] In the detection of target objects, it is necessary to acquire detailed information with high visual clarity by focusing and magnifying the objects.[15] Nevertheless, environmental constraints and uncertainties, such as uneven sunlight, external medium, and changeable weather conditions, often deteriorate contrast and clarity, and thus prohibit high-quality image acquisition (Figure 1c).[16−18] After obtaining image data, including the target object, it is imperative to recognize it efficiently and

Received: October 18, 2023
Revised: December 22, 2023
Accepted: December 27, 2023

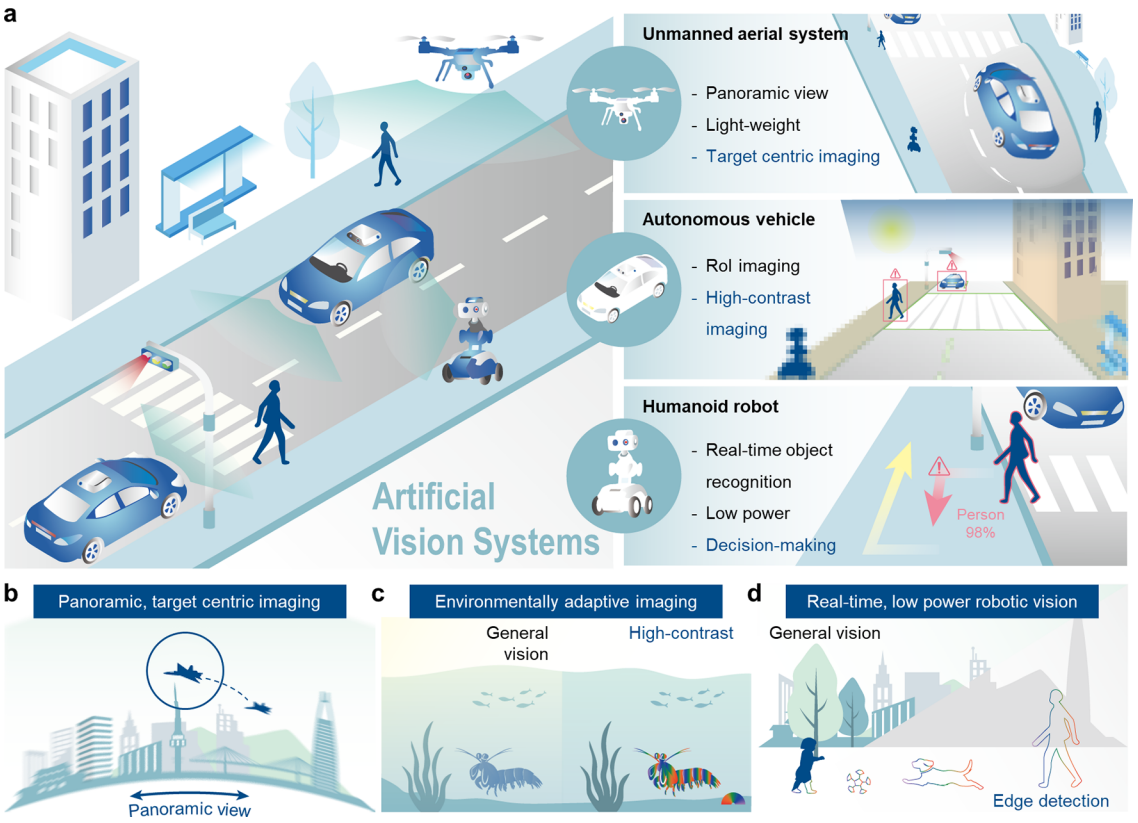

Figure 1. Artificial vision system for robotic vision. (a) Schematic illustration of robotic vision used in unmanned aerial systems, autonomous vehicles, and humanoid robots. The robotic visions capture, recognize, and interact with the nearby objects (e.g., humans, humanoid robots, cars, and drones) located in their region-of-interest (RoI). (b,c) Schematic illustration describing the application-specific imaging, such as panoramic and target-centric functionalities for effective object detection (b) and environmentally adaptive imaging capabilities for high-clarity image acquisition (c). (d) Schematic illustration showing the applications of robotic visions for enabling real-time and low-power decision-making.

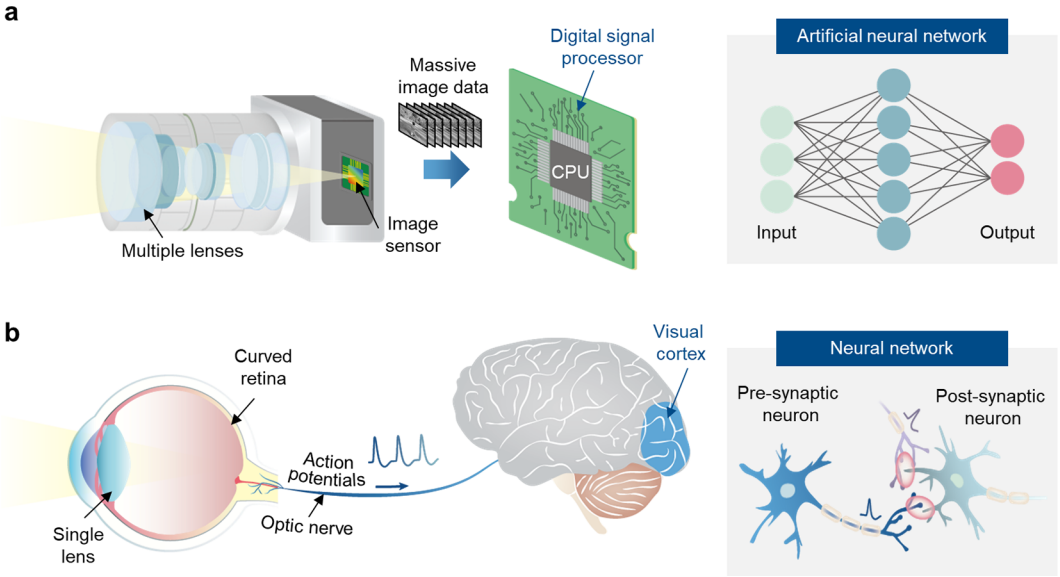

Figure 2. Imaging and data processing systems. (a) Traditional imaging and data processing systems, featuring a front-end camera equipped with a multilens system, a CMOS image sensor, and a back-end digital signal processor. The incident light is focused on the CMOS image sensor by multiple lenses and subsequently captured. The vast amount of image data is then transferred to digital signal processors for processing through machine learning algorithms based on artificial neural networks. (b) Human visual recognition system comprising an eye with a single lens and a curved retina and a brain with a visual cortex. The incident light is focused on the curved retina by a single lens, activating photoreceptor cells. Visual information is then transmitted to the visual cortex in the form of APs, and neural networks, consisting of numerous interconnected neurons via synapses, interpret this information.

https://doi.org/10.1021/acsnano.3c10181
ACS Nano XXXX, XXX, XXX−XXX

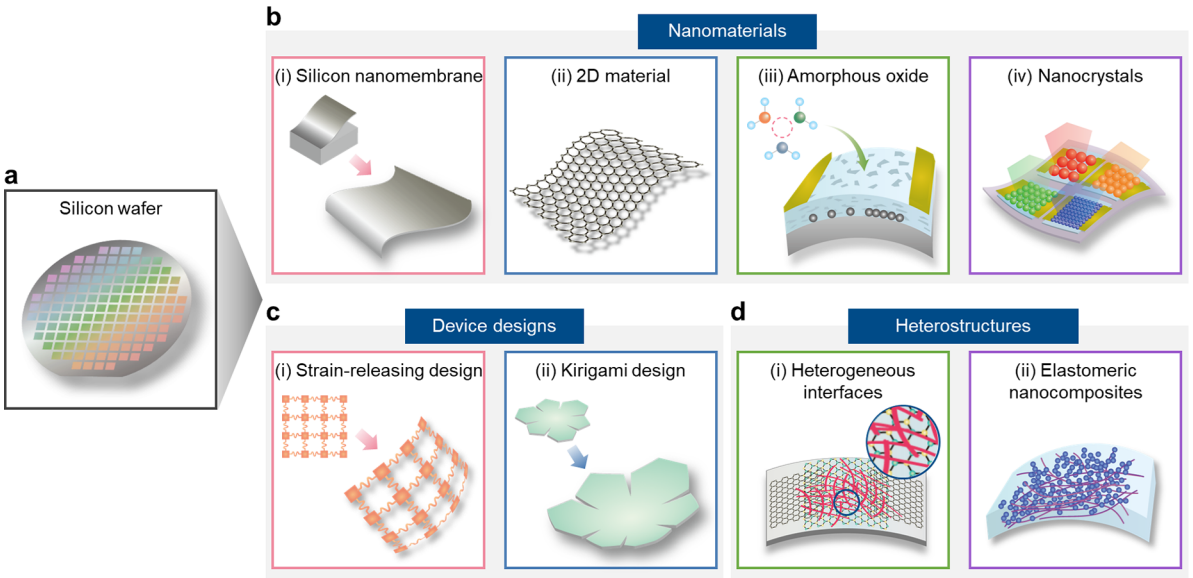

Figure 3. Nanotechnology for artificial vision systems. (a) Schematic illustration of a rigid and flat Si wafer employed in CMOS image sensors. (b–d) Nanotechnologies, including nanomaterials (b), device designs (c), and heterostructures (d), applied in the innovation of artificial vision systems. Various nanomaterials, such as silicon nanomembranes, 2D materials, amorphous oxide semiconductors, and nanocrystals, have been utilized in developing artificial vision systems. In particular, their collaborative synergy with device designs (e.g., strain-releasing designs and kirigami designs) and integration into heterostructures facilitate the advances in artificial vision systems.

swiftly.[19,20] However, this procedure involves processing a large amount of image data and needs significant power consumption and processing time,[21,22] which are incompatible with situations of rapidly moving mobile robots.[7] Thus, energy-efficient and time-efficient image data processing is crucial to enhance the decision-making capability of a mobile robot (Figure 1d).[23−25]

Conventional imaging systems, however, may not be ideal for mobile robotic visions due to their inherently bulky optical systems and inefficient data processing architectures (Figure 2a).[26,27] Traditional cameras require multilens optics to focus visual images onto a flat complementary metal-oxide-semiconductor (CMOS) image sensor array, which increases system complexity, size, and weight.[28] Achieving multifunctionality for application-specific imaging capabilities also demands the integration of bulky and heavy optical components into the camera module,[29,30] which can significantly reduce the mobility of the robots. Furthermore, the primary functions of conventional cameras prioritize image acquisition, necessitating additional high-performance processors and large energy storage devices,[20,31] neither of which are suitable for the desired compactness and lightweight for mobile robots.

Meanwhile, natural vision systems, from biological eyes to visual recognition systems, which oftentimes show excellent performance and simple structure by surpassing those of man-made vision systems, offer promising insights to address the inefficiencies of conventional devices (Figure 2b).[26,32] However, to mimic and implement key structural and functional features of the biological vision systems, it is required to realize curved form factors[33−35] and neuromorphic characteristics[36−38] in the imaging system. However, these cannot be achieved by using traditional rigid and flat CMOS image sensors.[21,31] Thereby, mechanically deformable nanomaterials (e.g., silicon (Si) nanomembranes,[34,39,40] two-dimensional (2D) materials,[41−44] amorphous oxide semiconductors,[45,46] and nanocrystals (quantum dots (QDs)[47,48] and halide perovskites[49−51])) and unconventional device technologies (e.g., flexible devices with kirigami designs,[33,34,39] devices using stretchable interconnections,[52−54] and intrinsically stretchable devices[47,55]) have emerged as promising technical solutions for the development of multifunctional high-performance bioinspired artificial vision systems.

Here, we review recent advances in the development of nanomaterial-based artificial vision systems, with a particular focus on bioinspired electronic eyes and in-sensor processing devices. We first present an overview of the technology progress in bioinspired artificial vision systems. We then discuss more details about the electronic eyes that structurally mimic biological eyes, such as single-chambered and compound eyes, by describing distinct aspects of their hardware components. Next, we explain in-sensor processing devices that functionally mimic animal visual recognition systems by describing how to process image signals at the image-sensor level and maximize the processing efficiency of the acquired image data. We also include a brief future outlook on bioinspired artificial vision systems by presenting insights for upcoming research directions, ideal system requirements, and potential future applications.

ARTIFICIAL VISION SYSTEMS BASED ON NANOMATERIALS

Nanoscale Materials and Device Design Strategies for Artificial Vision Systems. Nanomaterials, exhibiting unique electrical, optical, and mechanical properties due to their nanoscale dimensions, have huge potential in developing artificial vision systems by overcoming the constraints of conventional device technologies based on rigid, flat, and thick Si wafers (Figure 3a). For instance, single crystalline Si nanomembranes with submicrometer-scale thickness can withstand mechanical deformations without fracture while preserving their intrinsic electrical performance and processability found in bulk Si (Figure 3b, (i)).[53,56] 2D materials feature electrical conductivity and photoabsorption properties

https://doi.org/10.1021/acsnano.3c10181
ACS Nano XXXX, XXX, XXX−XXX

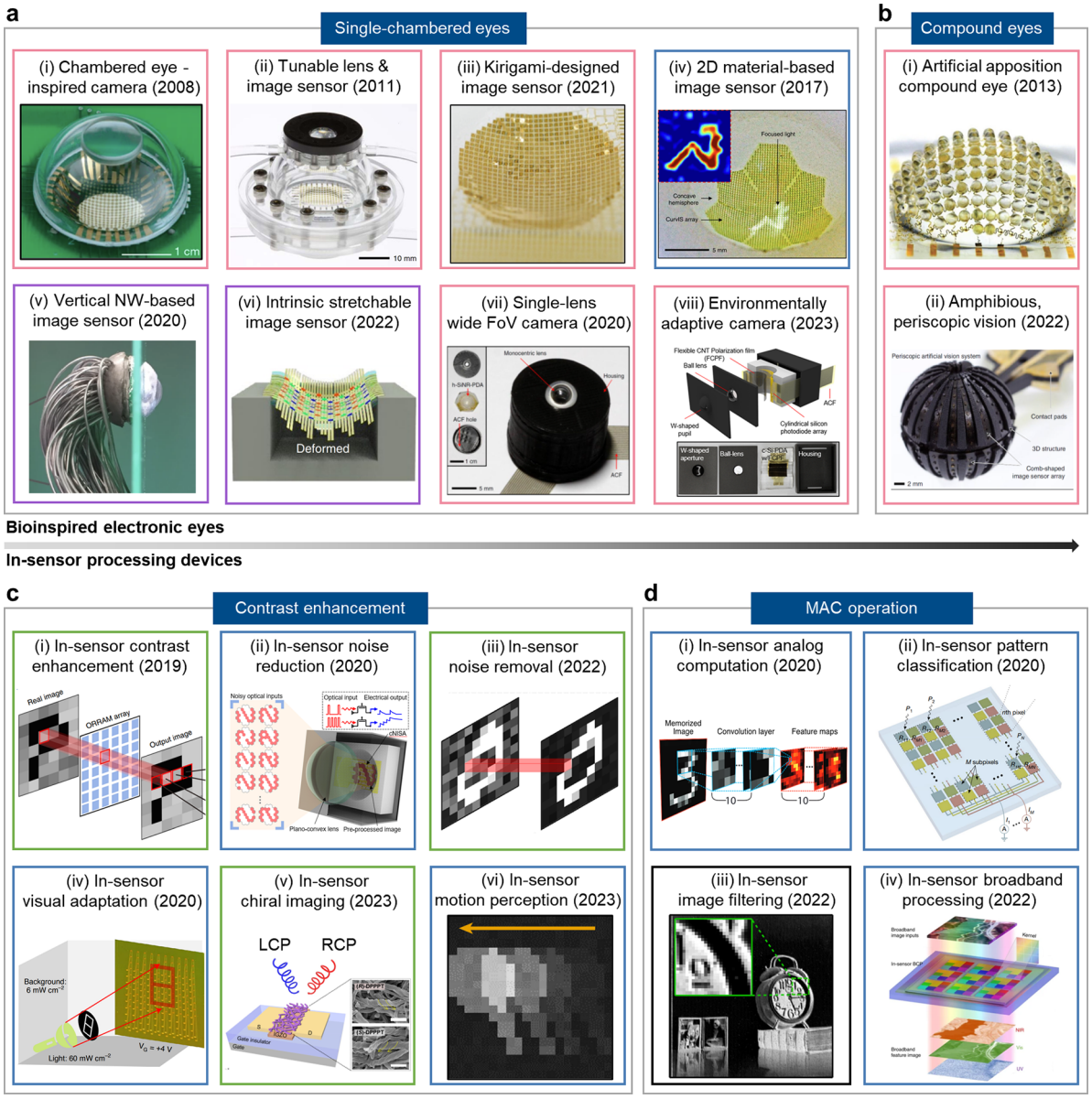

Figure 4. Recent advancement of artificial vision systems. (a–d) Recently developed bioinspired electronic eyes, e.g., the electronic eyes mimicking single-chambered eyes (a) and compound eyes (b), and in-sensor processing devices for performing contrast enhancement (c) and MAC operations (d) of image data. The colors of boxes represent the materials used; for example, red, blue, green, purple, and black boxes indicate the use of silicon nanomembranes, 2D materials, amorphous oxides, nanocrystals, and silicon wafers, respectively. Adapted with permission from ref 35. Copyright 2008 Nature Publishing Group (NPG). Adapted with permission from ref 40. Copyright 2011 National Academy of Sciences (NAS). Adapted with permission from ref 39. Copyright 2021 NPG. Adapted with permission under a Creative Commons CC License from ref 33. Copyright 2017 NPG. Adapted with permission from ref 72. Copyright 2020 NPG. Adapted with permission from ref 47. Copyright 2022 NPG. Adapted with permission from ref 14. Copyright 2020 NPG. Adapted with permission from ref 17. Copyright 2023 American Association for the Advanced Science (AAAS). Adapted with permission from ref 54. Copyright 2013 NPG. Adapted with permission from ref 77. Copyright 2022 NPG. Adapted with permission from ref 81. Copyright 2019 NPG. Adapted with permission under a Creative Commons CC License from ref 31. Copyright 2020 NPG. Adapted with permission under a Creative Commons CC License from ref 85. Copyright 2022 AAAS. Adapted with permission from ref 18. Copyright 2022 NPG. Adapted with permission under a Creative Commons CC License from ref 29. Copyright 2023 Wiley-VCH. Adapted with permission from ref 88. Copyright 2023 NPG. Adapted with permission from ref 10. Copyright 2020 Wiley-VCH. Adapted with permission from ref 19. Copyright 2020 NPG. Adapted with permission from ref 91. Copyright 2022 NPG. Adapted with permission from ref 30. Copyright 2022 NPG.

as well as exceptional mechanical flexibility due to their atomically thin thickness and quantum confinement effect (Figure 3b, (ii)).[57−59] Additionally, 2D materials are notable for their low power consumption,[36] enhancing their suitability for mobile applications. Photodetectors made of amorphous oxide thin films offer unconventional photoresponses similar to synaptic characteristics of natural vision systems because of their intrinsic carrier-trapping properties,[45,60,61] in addition to mechanical flexibility (Figure 3b, (iii)). Semiconducting nanocrystals (e.g., QDs[8,62,63] and halide perovskites[64−67]) hold the key for developing high-performance photodetectors owing to their high exciton generation efficiency, long carrier lifetime, and color tunability (Figure 3b, (iv)).

https://doi.org/10.1021/acsnano.3c10181
ACS Nano XXXX, XXX, XXX−XXX

These advantages of the nanomaterials can be amplified further, when the nanoscale material strategies are combined with unconventional device design strategies[1,54] and/or organic- or elastomer-based material strategies,[68−71] enabling the image sensors to have hemispherically curved form factors and/or neuromorphic characteristics. For example, strain-releasing designs (e.g., pop-up bridge structures[35] and serpentine interconnections[14,40]) can provide mechanical deformability to the devices (Figure 3c, (i)). Alternatively, kirigami designs compensate for the geometric difference between 2D substrates and three-dimensional (3D) structures, ensuring for the image sensors to have 3D configurations (Figure 3c, (ii)).[33,34] Meanwhile, organic dielectric layers integrated with 2D materials for a trap-rich interface increase the retention time of photocurrents and enable synaptic photoresponses (Figure 3d, (i)).[31,36] Intrinsically stretchable light-absorbing nanocomposites based on QDs and elastic block copolymers provide opportunities for artificial vision systems with dynamically tunable focus and multispectral imaging (Figure 3d, (ii)).[47]

Such properties of the engineered nanomaterials (e.g., mechanical deformability and synaptic property) have enabled the development of artificial vision systems. There have been two representative approaches toward highly efficient artificial vision systems: the development of bioinspired electronic eyes and the development of in-sensor processing devices. A brief review on the technology development history for each approach will be given in the following sections.

Recent Progress in Bioinspired Electronic Eyes. The first approach to developing highly efficient artificial vision systems involves emulating the structural features of animal eyes, which exhibit unique imaging capabilities despite their simple optical systems.[26,27] This effort led to the development of a human eye-inspired single-lens-based electronic eye, employing curved image sensor (CurvIS) arrays using Si nanomembranes (Figure 4a, (i)).[35] The shape of the CurvIS array matches that of the Petzval surface formed by the lens, allowing aberration-free imaging with single-lens optics. Furthermore, by introducing shape-tunability to the lens and CurvIS array, the electronic eye exploited the visual accommodation of the human eye (Figure 4a, (ii)).[40] Recently, the CurvIS array was designed to have a stretchable kirigami structure, allowing both shape-tunability for dynamic focus adjustment and a high fill factor for enhanced imaging resolution (Figure 4a, (iii)).[39]

In addition to Si nanomembranes, other nanomaterials have been integrated into CurvIS arrays, each offering unique advantages that surpass the constraints of traditional Si materials. For instance, the pixel density of CurvIS arrays could also be increased by adopting inherently deformable nanomaterials, such as 2D materials or perovskite nanowires (NWs) (Figure 4a, (iv−v)).[33,72] Perovskite NWs also showed higher photoabsorption properties than Si nanomembranes. Recently, visual accommodation and filter-free color detection could be simultaneously achieved by employing an intrinsically stretchable QD-nanocomposite-based CurvIS array (Figure 4a, (vi)).[47] By tuning the curvature of the array and adjusting the size of QDs, the focal length and absorption wavelength could be controlled.

Single-lens cameras have expanded their functionality by providing additional imaging capabilities and/or characteristics by mimicking features of aquatic animal eyes, such as fish and cuttlefish eyes (Figure 4a, (vii−viii)).[14,17] These functionalities include wide FoV, deep depth-of-field (DoF), self-equalization of nonuniform sunlight, and polarization recognition, all of which have the potential to significantly enhance imaging effectiveness during various robotic vision tasks under diverse environments. Additionally, the incorporation of two distinct electronic eyes, emulating the binocular vision of biological systems, can provide depth information,[73] facilitating stereoscopic robotic vision particularly beneficial for autonomous driving applications.

Compound eyes, which consist of an array of ommatidia (or facets) and can be found in insects or crustaceans, have also inspired the development of unconventional electronic eyes.[74,75] One of the representative electronic compound eye has been developed by integrating Si nanomembrane-based CurvIS arrays with polymeric microlenses arrays (MLAs). This electronic compound eye offered wide FoV and nearly infinite DoF imaging capabilities (Figure 4b, (i)).[54] In another example, Floreano et al. developed a Drosophila eye-inspired electronic compound eye by slicing a CMOS image sensor array and mounting them on a flexible printed circuit board.[76] This system could harness the benefits of compound eye systems and CMOS technologies. Recently, an amphibious and periscopic compound-eye-type artificial vision system was developed by mimicking flat corneal microlenses with graded refractive indices (RIs) of fiddler crab eyes (Figure 4b, (ii)).[77,78] The flat corneal MLA was integrated with a Si photodiode array and then mounted on a spherical substrate, which led to extremely wide FoV (>300 degrees) and amphibious imaging capability.

Recent Progress in In-Sensor Processing Devices. The second approach to developing highly efficient artificial vision systems involves embedding data processing function into the image sensor, aiming to perform image data processing at the image sensing stage by mimicking functional features of neurons and synapses in the human visual recognition system.[4] This technique is referred to as in-sensor processing (or in-sensor computing), which can decrease power consumption and improve bandwidth by deriving preprocessed data, without transferring vast amounts of image data over the entire time domain to the post-processor (i.e., we can transfer only a reduced size of data (preprocessed data) for post-processing).[25,79,80]

To achieve in-sensor processing, synaptic photodetectors that show unconventional photoresponses, such as time-dependent photocurrent generation and persistent photoconductivity, were developed by leveraging the material and interfacial properties of amorphous oxides and 2D materials (Figure 4c, (i−ii)).[31,81] These synaptic photodetectors enable in-sensor contrast enhancement, which reduces undesired background noise to improve image recognition rate.[82,83] Besides, neuronal properties of the leaky integrate-and-fire (LIF) mechanism[73,84] were mimicked by integrating a synaptic photodetector with a threshold-switching device (e.g., diode), in which background noise was filtered out while meaningful signals were significantly amplified (Figure 4c, (iii)).[85]

The synaptic photodetectors have also expanded their functions to exploit the visual adaptation function of the human retina (Figure 4c, (iv)).[18,68,86] This device showed a high-contrast image acquisition capability regardless of background illumination levels, demonstrating scotopic and photopic adaptation capabilities found in the human eye. In another example, the synaptic photodetector was employed in chiroptical imaging for selective identification of circularly

https://doi.org/10.1021/acsnano.3c10181
ACS Nano XXXX, XXX, XXX−XXX

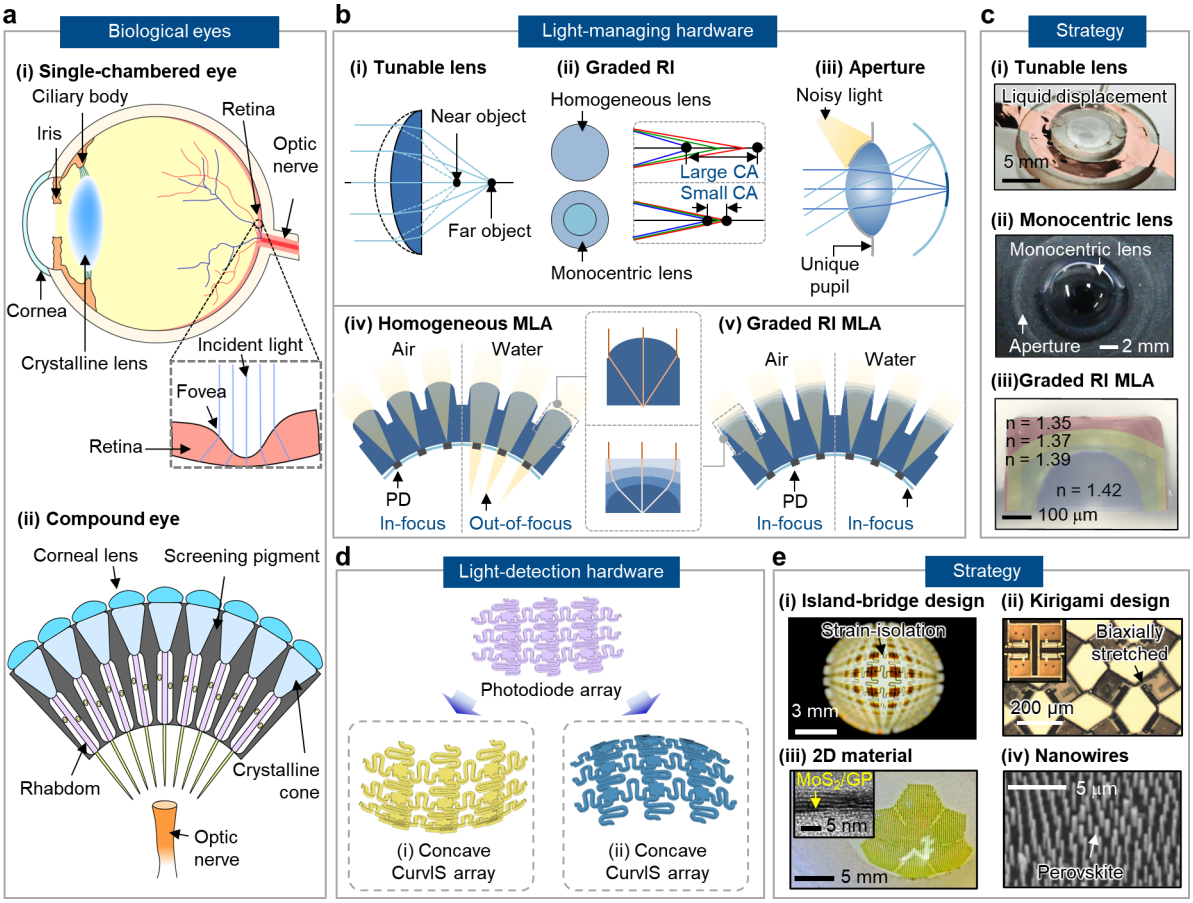

Figure 5. Bioinspired electronic eyes. (a) Schematic illustration of biological eyes: single-chambered eyes (i) and compound eyes (ii). (b) Light-managing components employed in bioinspired electronic eyes. (c) Examples of light-managing components, including shape-tunable lens (i), monocentric lens (ii), and graded RI MLA (iii), fabricated using polymer-based lens fabrication techniques. Adapted with permission under a Creative Commons CC License from ref 98. Copyright 2021 Wiley-VCH. Adapted with permission from ref 14. Copyright 2020 NPG. Adapted with permission from ref 77. Copyright 2022 NPG. (d) Light-detecting components, e.g., concavely and convexly curved photodetector arrays, used in bioinspired electronic eyes. (e) Strategies for realizing CurvIS array through applying unconventional device designs (e.g., strain-isolation device designs (i) and kirigami designs (ii)) and utilizing nanomaterials (e.g., 2D materials (iii) and perovskite NWs (iv)). Adapted with permission from ref 40. Copyright 2011 NAS. Adapted with permission from ref 39. Copyright 2021 NPG. Adapted with permission under a Creative Commons CC License from ref 33. Copyright 2017 NPG. Adapted with permission from ref 72. Copyright 2020 NPG.

polarized (CP) light with a specific rotating orientation (Figure 4c, (v)).[29,87] This synaptic photodetector amplified the photocurrent generated by frequent CP lights with the target orientation only, and thus, the selectivity could be improved. Recently, the application of synaptic photodetectors was expanded to dynamically moving objects for improving the efficiency of motion perception (Figure 4c, (vi)).[88] The object's moving direction could be inferred by utilizing the afterimages of moving objects, generated by synaptic photodetectors.

Meanwhile, a crossbar array of synaptic photodetectors can be used for the "multiply-accumulate" (MAC) operation (e.g., analog vector-matrix multiplications) for pattern recognition and image filtering (Figure 4d, (i)).[10] For instance, MAC operations ($I_n = \Sigma C_{m,n} \times V_m$) could be executed by programming their conductance values to represent target matrix elements and subsequently applying the voltages converted from the intensities of image patches to the crossbar array.[55,89,90] However, such analog processing necessitates power-/time-consuming steps for the acquisition, transmission, and conversion of image data.[91]

Therefore, alternatively, reconfigurable photodetectors, of which responsivity can be electrostatically tuned to match the matrix elements, were developed to perform MAC operations within the array itself (Figure 4d, (ii–iii)).[19,91] The array of reconfigurable photodetectors generated photocurrent, a direct output of the MAC operation between programmed responsivities and image intensities ($I_n = \Sigma R_{n,m} \times P_m$). Therefore, these reconfigurable photodetectors reduce data processing steps, improving the time and energy efficiency in image filtering and pattern recognition steps.[19,79] Recently, their functions expanded to broadband applications by employing the narrow bandgap 2D materials (e.g., $PdSe_2$ and $MoTe_2$).[30] These narrow bandgap 2D materials exhibited broadband photoresponses and thus allowed simultaneous acquisition and processing of broadband images through a single readout operation (Figure 4d, (iv)).

DETAILS ON BIOINSPIRED ELECTRONIC EYES

Structures and Optical Components of Biological Eyes. Recent advances in bioinspired electronic eyes have been driven by mimicking the structures and optical

https://doi.org/10.1021/acsnano.3c10181
ACS Nano XXXX, XXX, XXX−XXX

components of biological eyes, which confer distinct optical benefits to the artificial vision system. Biological eyes can be categorized into two types: single-chambered eyes and compound eyes.[26] The structures and functions of animal eyes have evolved in various ways, optimized for survival according to their habitat environment.[92]

First, the single-chambered eye typically comprises a crystalline lens, an iris, and a hemispherical retina (Figure 5a, (i)).[8] The crystalline lens focuses incident light onto the retina, and the iris blocks stray light while adjusting the pupil size according to ambient light levels.[93] The ciliary body dynamically alters the shape of the crystalline lens through its contraction and extension for focus adjustment. The retina has a concavely hemispherical structure, aligning with the Petzval surface of the crystalline lens.[33] Numerous photoreceptor cells (e.g., rod cells and cone cells) distributed on the retina generate electrophysiological signals in response to the light focused by the lens, enabling visual recognition.[27] A notable structure in the retina is the fovea, a central pit with densely packed cone cells, which is responsible for high visual acuity (Figure 5a, (i) inset).[94]

Second, the compound eye consists of multiple ommatidia, and a single ommatidium consists of a cornel lens, a crystalline cone, screening pigment, and rhabdom (Figure 5a, (ii)).[95] The corneal lens and crystalline cone collect incoming light, and the screening pigment filters the stray light that might interfere the light collection in adjacent rhabdoms as noise.[96] The photoreceptor cells located in the rhabdom are activated when exposed to incoming light. Each rhabdom functions as an individual detector that captures only a small portion of the overall image. This method of imaging enables quick and sensitive motion detection.

Despite the structural and functional differences between these two types of eyes, we cannot claim that one vision system is superior to the other. Rather, each possesses its own advantages and disadvantages. For instance, single-chambered eyes excel at high visual-acuity imaging, making them ideal for object recognition tasks.[72] Consequently, these eyes inspire the development of artificial vision systems capable of high-resolution, aberration-free, and environmentally adaptable imaging. On the other hand, compound eyes exhibit lower visual acuity than single-chambered eyes, but compensate for this limitation by offering extremely wide FoV, infinite DoF, and a compact form factor.[75] These characteristics make the electronic compound eyes highly suitable for surveillance applications, where extensive observation coverage for simultaneously detecting multiple objects is crucial.

Since each type of electronic eye has a distinct structure, the hardware design, resulting device performance, and their function are quite different. Each advantage/disadvantage can be carefully considered to be optimized and applied to specific robotic applications. In the following section, we will discuss recent advances in bioinspired electronic eyes, with a particular focus on light-managing and light-detecting hardware.

Light-Managing Components of Bioinspired Electronic Eyes. One of the key components of bioinspired electronic eyes is the light-managing hardware, whose designs and functions are emulated from biological lenses. In the case of early research for single-chamber-type electronic eyes, commercial lenses, such as a plano-convex lens and a ball lens, have been used.[35] Despite their cost benefits, these commercial lenses could not fully provide advantages of biological eyes. For instance, the shape of the crystalline lens in human eyes can be modified to adjust the focal length depending on the object distance.[97] Simple ray-tracing simulations show that a narrower crystalline lens results in a longer focal length due to the increased refraction angle at the lens surface (Figure 5b, (i)). However, achieving such a shape modification is not feasible with hard commercial lenses. Therefore, instead of commercial lenses, shape-tunable lens systems were developed by introducing polymer-based tunable lenses, whose shape could be changed through microfluidic or electromagnetic actuation (Figure 5c, (i)).[98,99] These lens systems varied the focal length by altering their shape, thus, enabling the focus adjustment for objects at different distances.

Another example is found in the case of crystalline lenses. Most crystalline lenses found in single-chambered eyes exhibit a gradient in the RI profile to compensate for optical aberrations.[27] In commercial lenses with homogeneous RI profiles, light dispersion occurs during its travel through the lens, resulting in different focal lengths for different wavelengths (Figure 5b, (ii) top). This is known as chromatic aberration (CA), which is often described as color distortion. But, if the gradient RI profile can be used, it can effectively compensate for the dispersion and significantly minimize CA (Figure 5b, (ii) bottom). Therefore, Kim et al. demonstrated a monocentric lens featuring graded RIs by assembling half-ball lenses and shell lenses with different RIs (Figure 5c, (ii)).[14] This monocentric lens proved to be highly effective in minimizing chromatic aberration. Furthermore, its spherically symmetric shape provided an additional advantage, enabling almost hemispherical FoV of up to 160°, much larger than conventional ellipsoidal lens systems.

In addition to the lens designs, the pupil shape in single-chambered biological eyes (e.g., cuttlefish eye) has been emulated to develop noise-robust robotic vision systems. For instance, the cuttlefish-inspired electronic eye has a W-shaped aperture mounted on a spherical ball lens, capable of correcting the uneven light distribution (Figure 5b, (iii)).[17] This situation can be made during the daytime, when intense sunlight comes from above. In that case, the uneven light can be self-equalized, as strong light coming from the top can be blocked by the aperture. This function is beneficial for autonomous driving under strong sunlight during the daytime.

For electronic eyes inspired by compound eyes, MLAs were developed, which were engineered to mimic the corneal lens and crystalline cone of compound eyes. Such MLAs were mounted onto the CurvIS arrays with the convex curvature, forming a focal plane on the CurvIS array by refracting incident light at their curved top surface (Figure 5b, (iv)).[54] This enables imaging without the need for bulky lens elements, required in aforementioned single-lens-based electronic eyes, leading to a small-form-factor while simultaneously achieving an extremely wide FoV (>160 degrees).

Initial versions of MLAs had a homogeneous RI profile to streamline the manufacturing process. These MLAs lose focusing capabilities if the external medium is changed between air and water due to RI changes (Figure 5b, (iv)), making them less suitable for amphibious robotic vision. To overcome this challenge, researchers developed a graded RI MLA with a flat top surface, inspired by the fiddler crab's eye that has flat corneal lenses and gradual RI layers.[77] The graded RI MLA with a flat top surface was fabricated by using a multistamp-and-curing process (Figure 5b, (v)). Each microlens consisted of four-layered optical adhesives with different RIs of 1.35, 1.37, 1.39, and 1.42, which were stacked in a

https://doi.org/10.1021/acsnano.3c10181
ACS Nano XXXX, XXX, XXX−XXX

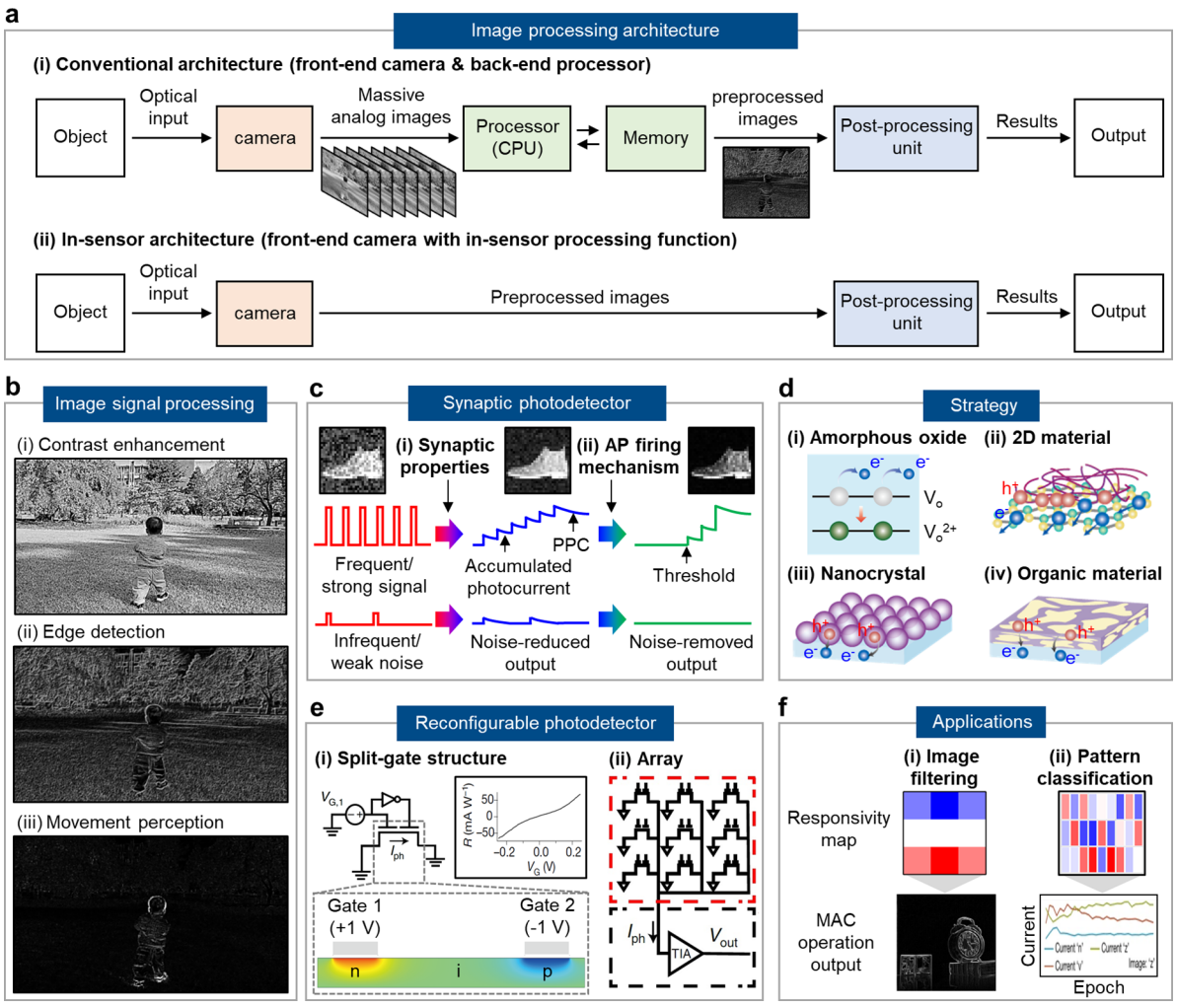

Figure 6. In-sensor processing devices. (a) Schematic diagram showing the imaging and data processing procedure in conventional architectures composed of front-end cameras and back-end processors (i) and in-sensor processing architectures composed of in-sensor processing devices (ii). (b) Representative examples of ISPs, such as contrast enhancement (i), edge detection (ii), and moving object tracking (iii), for improving the efficiency and accuracy of robotic vision tasks. (c) Photoresponses of synaptic photodetectors responding differently to frequent/strong signals and infrequent/weak noises. Adapted with permission under a Creative Commons CC License from ref 85. Copyright 2022 AAAS. (d) Physical phenomena observed in nanoscale materials and their heterostructures, including amorphous oxides (i), 2D materials (ii), nanocrystals (iii), and organic materials (iv), employed for developing synaptic photodetectors. (e) Device structure (i) and array configuration (ii) for constructing the reconfigurable photodetector arrays capable of executing MAC operations. (f) Application examples of analog MAC operations for robotic vision tasks, such as image filtering (i) and pattern classification (ii), achieved by the arrays of reconfigurable photodetectors. Adapted with permission from ref 91. Copyright 2022 NPG. Adapted with permission from ref 19. Copyright 2020 NPG.

curvilinear manner to create gradually changing RI layers (Figure 5c, (iii)). In this MLA, the flat top surface neutralized abrupt changes of focusing power at the interface between MLA and external medium (e.g., air or water), and the curvilinearly stacked polymeric layers with the gradient RI profile refracted the incident light to form a focal spot. Therefore, the electronic compound eye could maintain a consistent focal length in both aerial and underwater environments.

Light-Detecting Components of Bioinspired Electronic Eyes. Despite the significant advances in the light-managing components, their optical advantages remain underutilized until they are integrated with CurvIS arrays. In the case of single-lens-based electronic eyes, their imaging performance is constrained to a narrow FoV when employing the flat image sensor.[28] As the FoV broadens, a mismatch between the flat image sensor and the curved focal plane increases, resulting in an optical aberration known as Petzval field curvature. To resolve this challenge, a concave curvature, similar to the concavity of animal's retina, must be introduced to the photodiode array (Figure 5d, (i)). This concave curvature in the photodiode array enables alignment with the focal plane formed by the lens, ensuring an aberration-free imaging performance across wide FoVs.

In the electronic compound eye, it is crucial to position an individual photodiode at the focal point of each microlens. Thus, MLAs should be closely mounted onto the photodiodes, considering the short focal length of microlenses.[96] However, placing the MLA on a flat image sensor array severely restricts the FoV, preventing full exploitation of the optical benefits offered by compound eyes, such as extremely wide FoV. Therefore, MLAs should be integrated onto a CurvIS array with a convex configuration, resembling the convex hexagonal arrays found in natural compound eyes (Figure 5d, (ii)).

https://doi.org/10.1021/acsnano.3c10181
ACS Nano XXXX, XXX, XXX−XXX

In the early research reports, CurvIS arrays employed Si nanomembranes compatible with standard semiconductor manufacturing techniques such as CMOS fabrication processes.[35,40] These Si photodiode arrays were initially fabricated on a flat wafer and subsequently transferred onto concave or convex substrates for CurvIS arrays with concave or convex configurations.[100] Despite their submicrometer thickness, however, Si nanomembranes exhibit inherent brittleness, and thus strain-releasing device designs are necessary. For example, Si photodetector arrays were patterned into specific designs (e.g., island-bridge configuration) to minimize induced strain on the Si nanomembrane in CurvIS arrays by releasing most of the strain at the deformable metal interconnections (e.g., serpentine-shape interconnection; Figure 5e, (i)).

However, these strain-isolation device designs lead to low fill factors of photodetectors (~30%) because substantial space of the array is occupied by the specially designed interconnection.[33] Kirigami techniques, facilitating deformation of a 2D sheet into a 3D structure by adding cuts, can be a potential solution to achieve both a high fill factor and 3D deformation. By employing a hinge design in the photodetector array, for example, a CurvIS array which shows a fill factor of ~78% and biaxial stretchability could be developed (Figure 5e, (ii)).[39] This CurvIS array allowed both high-resolution imaging (32 × 32 pixels) and dynamic focus adjustment by being integrated with a shape-tunable lens system.

Recently, nanomaterials, such as 2D materials, perovskite NWs, and QD-based nanocomposites, have been used for CurvIS arrays because of their inherent deformability and unique material properties originating from nanoscale dimensions. These nanomaterial-based devices can be transferred from a manufacturing wafer to a curved substrate without mechanical failure, despite the lack of strain-isolation device designs, thus high pixel density can be achieved.[101] For example, a CurvIS array based on MoS_2-graphene heterostructure showed high pixel density because space-occupying device designs were unnecessary (Figure 5e, (iii)).[33] Another CurvIS array utilizing vertically grown perovskite NWs featured high NW density (~4.6×10^8 cm^{-2} with a pitch of 500 nm) that surpasses the photoreceptor density of the human retina (~10^7 cm^{-2} with a pitch of 3 μm) (Figure 5e, (iv)).[72] By utilizing nanocomposites of QDs, semiconducting polymers, and elastomeric matrix, an intrinsically stretchable image sensor array, facilitating the dynamic deformation of CurvIS array to align with the Petzval surface formed by the shape-tunable lens, can be fabricated.[47] Moreover, these nanomaterials exhibit high photoabsorption coefficients and long carrier diffusion lengths, enabling the fabrication of high-performance electronic eyes.

DETAILS ON IN-SENSOR PROCESSING DEVICES

Architecture of In-Sensor Processing Devices. In addition to image acquisition, energy- and time-efficient processing of the image data are crucial for successful robotic vision tasks. However, traditional image processing architectures, which rely on frame-based image acquisition, transfer of a large amount of image data, and subsequent data processing, have limitations in terms of power consumption and data latency.[102,103] In these architectures, a front-end camera captures individual image frames over a time period, by which a large amount of data should be accumulated in consideration of entire time domain (Figure 6a, (i)).[31] The data should be transferred to and processed by back-end processors for image analysis and recognition. However, these massive data transfer and processing cause latency and computational overhead, which are burdensome steps in the overall workflow of the robotic vision tasks.[104]

Image signal processing (ISP) techniques have improved data transfer and processing performances by preprocessing image data before it reaches to the post-processing stage.[20] One notable ISP technique is to emphasize key features of target objects through contrast enhancement (Figure 6b, (i)). This enables artificial intelligence to recognize a target object with high accuracy. This is particularly valuable when the initial image is noisy or blurred, which machine learning algorithms cannot recognize accurately without further processing.[85] Another ISP technique, e.g., edge detection, enhances data transfer efficiency by removing background information that may be unnecessary for object detection but occupies a large part of data storage (Figure 6b, (ii)).[79] In many cases, detecting the outlines of objects is sufficient for object detection.[5] In a more extreme case, tracking moving objects only, rather than capturing an entire scene that includes static backgrounds, can maximize the efficiency (Figure 6b, (iii)), as far as simplified image data is enough for the object tracking purpose.[12]

However, traditional architectures rely on back-end processors for ISP, in which inefficiency associated with the capture and transfer of massive data is accompanied. In this regard, in-sensor processing techniques hold a huge potential to significantly improve the overall efficiency by executing ISP at the image-sensor level (Figure 6a, (ii)).[21] However, conventional CMOS image sensors and readout integrated circuits have not been designed to support in-sensor processing. To implement in-sensor processing, data processing functions should be embedded into the image-sensing platform, and thus, unconventional photodetectors whose characteristics and configurations are different from CMOS image sensors are needed. In the following section, we will discuss recently highlighted in-sensor processing devices (e.g., synaptic photodetectors and reconfigurable photodetectors) and their applications to machine vision.

Synaptic Photodetector for In-Sensor Contrast Enhancement. The concepts of synaptic photodetectors draw inspiration from the neural signal transmission principle in the human visual recognition system, where action potentials (APs) propagate from presynaptic neurons to postsynaptic neurons via their synapse. In the synapse, the arrival of presynaptic APs triggers the release of neurotransmitters (e.g., glutamate), which in turn generates a postsynaptic potential through binding to receptors on the postsynaptic neuron. Subsequently, postsynaptic potentials are spatiotemporally accumulated, and an AP is fired when the summed potential exceeds the threshold.[105]

Synaptic photodetectors aim to integrate an ISP function by replicating such synaptic signal transmission characteristics.[45] To achieve this goal, photodetectors with slow photodynamic features (e.g., time-dependent photocurrent generation and persistent photoconductivity) were developed.[31,81,106] Their photoresponses resemble postsynaptic potentials in human synapses, i.e., accumulation of photocurrent in response to frequent and strong optical inputs and dissipation of photocurrent in response to infrequent and weak optical inputs (Figure 6c, (i)). As meaningful optical signals are usually frequent/repetitive and strong, while background noise tends to be infrequent/random and weak, these characteristics

https://doi.org/10.1021/acsnano.3c10181
ACS Nano XXXX, XXX, XXX−XXX

can be exploited to reduce background noise and amplify object signal, which leads to contrast enhancement of the image.[31]

Even with the noise-reduction technique, however, some residual background noise may persist, acting as an artifact that hinders accurate image recognition. To address this challenge, an advanced synaptic photodetector with threshold switching characteristics, more similar to a human synapse with an all-or-none type AP firing mechanism than the conventional synaptic photodetector, was developed.[85] In this device, a synaptic photodetector is integrated with a rectifying diode, and thus, an electrical output is generated only when it exceeds a turn-on threshold of the diode (Figure 6c, (ii)). When exposed to noisy inputs, this device generated negligible photocurrent. In contrast, it generated exponentially amplified photocurrent for meaningful input signals. The resulting noise-removed image could be accurately recognized by the machine learning algorithm through a single readout operation. The synaptic photodetector can also be used for tracking a moving object.[88] If the object continues to move, afterimages are produced due to the persistent photoconductivity. Furthermore, the new location of the moving object appears brighter in the images, including afterimages. Leveraging the brightness difference among these images enables us to infer the object's movement direction.

However, achieving such features using conventional Si photodiodes with fast photodynamics (i.e., rapid photocurrent generation and decaying characteristics) is challenging, even though defects are introduced.[107] In this regard, nanomaterials and their heterostructures have emerged as promising material candidates because their physical phenomena inducing photocurrent generation and relaxation gradually occur over a relatively long period of time due to the large activation energy. These physical phenomena enable nanomaterial-based photodetectors to exhibit synaptic photoresponses. In the case of amorphous oxide semiconductors (e.g., amorphous indium gallium zinc oxide (a-IGZO)), for instance, oxygen vacancies need to undergo ionization and deionization to generate and relax photocurrent, which leads to slow photodynamics (Figure 6d, (i)).[45,81] Another example that shows the slow photodynamics is the phototransistor with interfacial hole trapping/detrapping, which occurs at the interface of 2D materials and the organic dielectric layer (Figure 6d, (ii)).[18,31] Also, heterointerfacial charge transfer leads to time-dependent photocurrent generation and decaying characteristics. In nanocrystal-based heterostructures, for example, photogenerated electrons in nanocrystals (e.g., CdSe QDs) are transferred to semiconducting channels (e.g., a-IGZO channel) to generate photocurrent (Figure 6d, (iii)).[62,104] A similar heterointerfacial charge transfer mechanism is also found in the heterostructure of amorphous oxide semiconductors and organic semiconductor materials (Figure 6d, (iv)).[29]

Therefore, nanomaterials have been extensively studied to develop synaptic photodetectors as an alternative to single-crystalline Si. There will be numerous future endeavors exploring a wider array of nanomaterials and their heterostructures for advancing synaptic photodetectors.

Reconfigurable Photodetectors for the Multiply-Accumulate Operation. The MAC operation, commonly referred to as vector-matrix multiplication, is a popular computation scheme in machine vision applications, deriving output vectors through convolutional computations between matrices and vectors.[89] For example, an edge of the target object can be detected by applying the MAC operation between a 3×3 sobel$_x$ kernel (i.e., $[(-1, -2, -1), (0, 0, 0), (1, 2, 1)]$) and a 3×3 image patch.[60] Mapping the outputs obtained by sliding the original image patches and repeating the MAC operations results in an edge-extracted image. Machine learning also relies on the MAC operation, in terms of multiplication between a weight matrix and an input vector.[57]

Traditionally, these MAC operations were carried out through software-based calculation. However, this requires substantial computing resources and power consumption, which is problematic in mobile robotics applications for which low-power, real-time processing is crucial. Therefore, research efforts have been focused on executing the MAC operation in an analogue manner, bypassing traditional power-consuming computations.

For instance, the memristor crossbar array can produce current outputs that represent the outcome of the MAC operation between a conductance matrix and an input voltage vector ($I_n = \Sigma C_{n,m} \times V_m$).[55,90] In that case, the conductance of individual memristors is reconfigured to reflect the target filtering kernel or weight matrix, and the input image's intensities are converted into voltage signals and applied to the crossbar array. Similarly, the crossbar array comprised of synaptic photodetectors, whose conductance can be modulated through optical and/or electrical stimuli, was proposed for analog MAC operations.[10,108] However, this conductance-based method may not be ideal, because it necessitates additional signal processing steps such as recording, transmission, and signal conversion of image data before they are fed into the crossbar array.

The in-sensor processing aims to process image data at the image-sensing level, such as execution of the MAC operation in response to light illumination without additional signal processing steps. To achieve this goal, two fundamental factors are necessary. First, there should be well-defined physical parameters that can convert light intensities to electrical outputs through vector-matrix multiplication. For instance, the photocurrent is expressed as the product of photodetector's responsivity and incident light intensity ($I_{ph} = R \times P$). Second, these physical parameters, especially responsivity in this context, should be reconfigurable to represent elements in the desired filtering kernels or weight matrices. With these attributes, the MAC operation can be achieved in response to light illumination by programming responsivity matrices of individual pixels and summing the resulting photocurrents ($I = \Sigma R_{n,m} \times P_m$).

To realize such a reconfigurable photodetector, the split-gate device structure was proposed, offering the capability to program the responsivity of each pixel through electrostatic doping (Figure 6e, (i)).[19,91] In this device structure, the charge carrier profile within the semiconducting channel undergoes significant changes when an electric field is applied to the channel by the gate bias (Figure 6e, (i) gray dashed box). Notably, nanomaterials have gained significant attention as channel materials because of their large responsiveness to the applied electric field. For instance, 2D materials are highly susceptible to nearby electrical fields owing to their atomically thin nature.[19,30] Similarly, the intrinsic Si nanomembrane could also be used for the channel material.[91]

The split-gate devices, incorporating either 2D materials or Si nanomembranes, can be programmed to represent target responsivities corresponding to filtering kernels or weight matrix elements. Then, the source/drain electrodes of these

https://doi.org/10.1021/acsnano.3c10181
ACS Nano XXXX, XXX, XXX−XXX

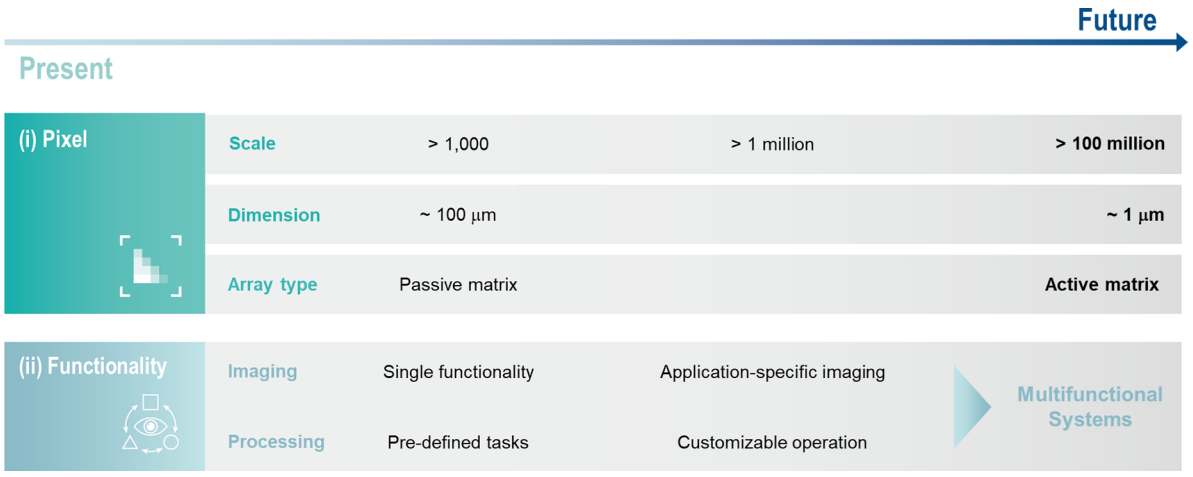

Figure 7. Technical roadmap for future artificial vision systems. Technical challenges for advancing artificial vision systems for robotic application. First, pixel density should be enhanced to levels comparable to CMOS image sensor arrays, necessitating miniaturization of the pixel dimension and adopting active-matrix array architectures. Second, the integration of functionalities between bioinspired electronic eyes and in-sensor processing devices is imperative. Moreover, customizing their functionalities to cater to specific robotic scenarios enables the development of versatile and multifunctional robotic vision systems.

devices were electrically interconnected, forming an array primed for conducting analogue MAC operations in response to patterned light (or image) illuminations (Figure 6e, (ii)). For instance, the responsivities of 3 × 3 device arrays were programmed with a sobel$_x$ kernel, and an output current, which is a summation of photocurrent generated from every pixel, was measured ($I_{ph} = \Sigma I_n$). This output current indicates the outcome of the multiplication and accumulation of the responsivity matrix and incident image patch ($I_{ph} = \Sigma R_n \times P_n$), which can be employed to construct an edge-detected image (Figure 6f, (i)).[91] Furthermore, classification of three different patterns could be achieved by using three subpixel arrays of reconfigurable photodetectors. The responsivity of each photodetector was optimized through back-propagation algorithms, and input optical patterns were inferred by comparing the output current from each subpixel array (Figure 6f, (ii)).[19]

CONCLUSION AND FUTURE PROSPECTS

We discussed recent advancements in artificial vision systems based on nanomaterials for robotic applications. The bioinspired electronic eyes have presented unique image acquisition performances due to their unconventional structures emulating biological eyes as well as the incorporation of nanomaterials with inherent deformability. The in-sensor processing devices have provided efficient hardware-centric approaches for ISPs, such as contrast enhancement and image filtering, which reduce data redundancy and lower power consumption of the robotic vision systems. Hence, artificial vision systems based on nanomaterials are expected to contribute to the advancement of mobile robotic visions that require superior imaging and recognition efficiency compared to traditional CMOS technologies. Despite these advances, however, there are still remaining challenges. In the final section, these challenges are briefly discussed, particularly focusing on the improvement of imaging resolution and integration of multiple functions.

Resolution Enhancement of the Artificial Vision System. Despite recent efforts to enhance the pixel density of the CurvIS array, the resolution of artificial vision systems is significantly lower than that of state-of-the-art CMOS image sensors. The low imaging resolution can constrain the practical use of artificial vision systems in robotic vision tasks. Therefore, a pressing need exists to increase the pixel density (Figure 7, (i)). To achieve this goal, the dimension of the individual pixel, which encompasses the active photodiode area and its spatial separation area, should be dramatically reduced. This size reduction of the pixel, however, cannot be achieved using strain-releasing device designs (e.g., strain-releasing serpentine structures). These designs necessitate substantial area to be occupied by spaces for interconnections and thus limit the fill factor.[33,39]

The ideal solution involves the development of an intrinsically stretchable image sensor array that can be mounted on a curved substrate with almost 100% fill factor, while potential risks of device fracture can be avoided. Nanomaterials exhibiting inherent flexibility and their composites with elastomeric materials can be promising material candidates for such image sensors. However, their practical implementation in a high-resolution array format is still a daunting goal because of the lack of facile fabrication methods and low device uniformity. Therefore, further advances in material preparation and fabrication techniques are imperative. Besides, the shrinkage of the design rule, while nanomaterials and their composites are employed, may cause crosstalk issues among neighboring pixels. Therefore, better multiplexing technologies are needed. This means that high-performance and intrinsically stretchable transistor technologies should be developed.[109]

Integration of Multiple Functions into a Single Device. Robotic vision tasks routinely encounter various environmental constraints and uncertainties, each demanding specialized imaging and processing capabilities tailored to specific applications. However, employing multiple, discrete imaging and processing devices to meet those diverse requirements is inefficient as well as makes the entire system complicated and bulky.[21] Instead, the key lies in integrating multiple functions into a single-integrated system, enhancing the efficiency, versatility, and mobility of robotic vision systems (Figure 7, (ii)).

https://doi.org/10.1021/acsnano.3c10181
ACS Nano XXXX, XXX, XXX−XXX

For this goal, tunable hardware components can be used, rendering them adaptable to various environments and applications. For instance, a wide FoV is beneficial for wide-range surveillance and target object detection. Consequently, a lens may have a spherical core−shell structure to support wide observation FoV.[14] However, once a target is detected, the system operation type can be changed to a zoom-in mode for detailed analyses, ensuring accurate identification. In that case, the optical system parameters should be adjustable for the zooming capability. In the case when uneven light intensity (e.g., sunlight) increases light scattering and thus hinders effective image acquisition, it becomes necessary to adapt the aperture shape and size for self-equalization.[17] These dynamic adjustments of imaging hardware components necessitate material and mechanical engineering. Other sensing components to improve vision performance can also be considered to be combined with imaging devices. Such sensors (temperature, humidity, air pollution quality, etc.) may be used to adjust the detailed parameters of the vision system. Certainly, all of these engineered components should be monolithically integrated within a single robotic vision system.

In-sensor processing functions should also be adjustable, enabling customization based on specific objectives. This adaptability ensures that in-sensor processing is not restricted to a predefined task but can handle various ISP operations, according to specific needs. For example, if we consider a general surveillance scenario requiring the detection and identification of moving objects, the detection of moving objects can be efficiently achieved by edge detection, by reducing data redundancy and handling fewer data. However, once a target is specified, highly accurate identification becomes essential, and thus, the in-sensor processing function should prioritize acquiring detailed image information for enhanced contrast. This adaptability of the vision system can be attained when the physical parameters (e.g., responsivity) of individual in-sensor processing devices are programmable to the desired ISP modes upon demand.

Future Prospects. Robotic vision tasks encompass multiple stages, such as image acquisition and ISP to include data analysis and decision making. These discrete stages, often handled by separate hardware components, result in substantial data flow between them and thus limit the efficiency of the robotic vision. However, it is crucial to note that the ultimate goal of robotic vision is the efficient acquisition and processing of image data for targeted applications. Considering this goal, we had better execute all those processes in a single-integrated device and one streamlined operation.[110] This necessitates the integration of all imaging and processing functions into one artificial vision system. Then, artificial vision systems can achieve high-quality imaging with a CurvIS array paired with simplified and miniaturized optical components and autonomously perform ISP with in-sensor processing capabilities. Ideally, back-end processors responsible for post-data processing, such as machine learning-based object inference, can also be monolithically integrated for low-power and high-speed robotic vision applications.[25] Therefore, the entire robotic vision process, from image acquisition to data analysis, can be performed in a unified and efficient manner, significantly enhancing the overall efficiency. While technical challenges persist, recent advancements in bioinspired electronic eyes and in-sensor processing devices are promising for high-performance robotic vision systems toward advanced mobile and human-friendly robotics.

AUTHOR INFORMATION

Corresponding Authors

Young Min Song − *School of Electrical Engineering and Computer Science and AI Graduate School, Gwangju Institute of Science and Technology, Gwangju 61005, Republic of Korea; Department of Semiconductor Engineering, Gwangju Institute of Science and Technology, Gwangju 61005, Republic of Korea;* orcid.org/0000-0002-4473-6883; Email: ymsong@gist.ac.kr

Dae-Hyeong Kim − *Center for Nanoparticle Research, Institute for Basic Science (IBS), Seoul 08826, Republic of Korea; School of Chemical and Biological Engineering, Institute of Chemical Processes, Seoul National University, Seoul 08826, Republic of Korea;* orcid.org/0000-0002-4722-1893; Email: dkim98@snu.ac.kr

Authors

Changsoon Choi − *Center for Optoelectronic Materials and Devices, Post-silicon Semiconductor Institute, Korea Institute of Science and Technology (KIST), Seoul 02792, Republic of Korea;* orcid.org/0000-0002-0428-5117

Gil Ju Lee − *Department of Electronics Engineering, Pusan National University, Busan 46241, Republic of Korea*

Sehui Chang − *School of Electrical Engineering and Computer Science, Gwangju Institute of Science and Technology, Gwangju 61005, Republic of Korea*

Complete contact information is available at: https://pubs.acs.org/10.1021/acsnano.3c10181

Author Contributions

¶C. Choi, G. J. Lee, and S. Chang contributed equally to this work.

Notes

The authors declare no competing financial interest.

ACKNOWLEDGMENTS

This research was supported by IBS-R006-A1. This research was also supported by the National Research Foundation of Korea grant funded by the Korean government (MSIT) (RS-2023-00209466, RS-2023-00217312), by the "Regional innovation mega project" program through the Korea Innovation Foundation funded by Ministry of Science and ICT (2023-DD-UP-0015), and the Future Resource Research Program of the Korea Institute of Science and Technology (KIST).

REFERENCES

(1) Luo, Y.; Abidian, M. R.; Ahn, J. H.; Akinwande, D.; Andrews, A. M.; Antonietti, M.; Bao, Z.; Berggren, M.; Berkey, C. A.; Bettinger, C. J.; Chen, J.; Chen, P.; Cheng, W.; Cheng, X.; Choi, S. J.; Chortos, A.; Dagdeviren, C.; Dauskardt, R. H.; Di, C. A.; Dickey, M. D.; Duan, X.; Facchetti, A.; Fan, Z.; Fang, Y.; Feng, J.; Feng, X.; Gao, H.; Gao, W.; Gong, X.; Guo, C. F.; Guo, X.; Hartel, M. C.; He, Z.; Ho, J. S.; Hu, Y.; Huang, Q.; Huang, Y.; Huo, F.; Hussain, M. M.; Javey, A.; Jeong, U.; Jiang, C.; Jiang, X.; Kang, J.; Karnaushenko, D.; Khademhosseini, A.; Kim, D.-H.; Kim, I. D.; Kireev, D.; Kong, L.; Lee, C.; Lee, N. E.; Lee, P. S.; Lee, T. W.; Li, F.; Li, J.; Liang, C.; Lim, C. T.; Lin, Y.; Lipomi, D. J.; Liu, J.; Liu, K.; Liu, N.; Liu, R.; Liu, Y.; Liu, Y.; Liu, Z.; Liu, Z.; Loh, X. J.; Lu, N.; Lv, Z.; Magdassi, S.; Malliaras, G. G.; Matsuhisa, N.; Nathan, A.; Niu, S.; Pan, J.; Pang, C.; Pei, Q.; Peng, H.; Qi, D.; Ren, H.; Rogers, J. A.; Rowe, A.; Schmidt, O. G.; Sekitani, T.; Seo, D. G.; Shen, G.; Sheng, X.; Shi, Q.; Someya, T.; Song, Y.; Stavrinidou, E.; Su, M.; Sun, X.; Takei, K.; Tao, X. M.; Tee, B. C. K.; Thean, A. V. Y.; Trung, T. Q.; Wan, C.; Wang, H.; Wang, J.; Wang, M.; Wang, S.; Wang, T.; Wang, Z. L.; Weiss, P. S.; Wen, H.; Xu, S.; Xu, T.; Yan, H.;

https://doi.org/10.1021/acsnano.3c10181
ACS Nano XXXX, XXX, XXX−XXX

Yan, X.; Yang, H.; Yang, L.; Yang, S.; Yin, L.; Yu, C.; Yu, G.; Yu, J.; Yu, S. H.; Yu, X.; Zamburg, E.; Zhang, H.; Zhang, X.; Zhang, X.; Zhang, X.; Zhang, Y.; Zhang, Y.; Zhao, S.; Zhao, X.; Zheng, Y.; Zheng, Y. Q.; Zheng, Z.; Zhou, T.; Zhu, B.; Zhu, M.; Zhu, R.; Zhu, Y.; Zhu, Y.; Zou, G.; Chen, X. Technology Roadmap for Flexible Sensors. *ACS Nano* **2023**, *17*, 5211−5295.

(2) Floreano, D.; Wood, R. J. Science, Technology and the Future of Small Autonomous Drones. *Nature* **2015**, *521*, 460−466.

(3) Jayachandran, D.; Oberoi, A.; Sebastian, A.; Choudhury, T. H.; Shankar, B.; Redwing, J. M.; Das, S. A Low-Power Biomimetic Collision Detector Based on an in-Memory Molybdenum Disulfide Photodetector. *Nat. Electron.* **2020**, *3*, 646−655.

(4) Wan, T.; Shao, B.; Ma, S.; Zhou, Y.; Li, Q.; Chai, Y. In-Sensor Computing: Materials, Devices, and Integration Technologies. *Adv. Mater.* **2023**, *35*, 2203830.

(5) Zhang, Z.; Wang, S.; Liu, C.; Xie, R.; Hu, W.; Zhou, P. All-in-One Two-Dimensional Retinomorphic Hardware Device for Motion Detection and Recognition. *Nat. Nanotechnol.* **2022**, *17*, 27−32.

(6) Wu, P.; He, T.; Zhu, H.; Wang, Y.; Li, Q.; Wang, Z.; Fu, X.; Wang, F.; Wang, P.; Shan, C.; Fan, Z.; Liao, L.; Zhou, P.; Hu, W. Next-Generation Machine Vision Systems Incorporating Two-Dimensional Materials: Progress and Perspectives. *InfoMat* **2022**, *4*, e12275.

(7) Choi, C.; Seung, H.; Kim, D.-H. Bio-Inspired Electronic Eyes and Synaptic Photodetectors for Mobile Artificial Vision. *IEEE Journal on Flexible Electronics* **2022**, *1*, 76−87.

(8) Kim, S.; Choi, Y. Y.; Kim, T.; Kim, Y. M.; Ho, D. H.; Choi, Y. J.; Roe, D. G.; Lee, J. H.; Park, J.; Choi, J. W.; Kim, J. W.; Park, J. H.; Jo, S. B.; Moon, H. C.; Jeong, S.; Cho, J. H. A Biomimetic Ocular Prosthesis System: Emulating Autonomic Pupil and Corneal Reflections. *Nat. Commun.* **2022**, *13*, 6760.

(9) Long, Z.; Qiu, X.; Chan, C. L. J.; Sun, Z.; Yuan, Z.; Poddar, S.; Zhang, Y.; Ding, Y.; Gu, L.; Zhou, Y.; Tang, W.; Srivastava, A. K.; Yu, C.; Zou, X.; Shen, G.; Fan, Z. A Neuromorphic Bionic Eye with Filter-Free Color Vision Using Hemispherical Perovskite Nanowire Array Retina. *Nat. Commun.* **2023**, *14*, 1972.

(10) Jang, H.; Liu, C.; Hinton, H.; Lee, M. H.; Kim, H.; Seol, M.; Shin, H. J.; Park, S.; Ham, D. An Atomically Thin Optoelectronic Machine Vision Processor. *Adv. Mater.* **2020**, *32*, 2002431.

(11) Ma, S.; Wu, T.; Chen, X.; Wang, Y.; Ma, J.; Chen, H.; Riaud, A.; Wan, J.; Xu, Z.; Chen, L.; Ren, J.; Zhang, D. W.; Zhou, P.; Chai, Y.; Bao, W. A 619-Pixel Machine Vision Enhancement Chip Based on Two-Dimensional Semiconductors. *Sci. Adv.* **2022**, *8*, eabn9328.

(12) Posch, C.; Serrano-Gotarredona, T.; Linares-Barranco, B.; Delbruck, T. Retinomorphic Event-Based Vision Sensors: Bioinspired Cameras with Spiking Output. *Proceedings of the IEEE* **2014**, *102*, 1470−1484.

(13) Lee, G. J.; Nam, W. Il; Song, Y. M. Robustness of an Artificially Tailored Fisheye Imaging System with a Curvilinear Image Surface. *Opt. Laser. Technol.* **2017**, *96*, 50−57.

(14) Kim, M. S.; Lee, G. J.; Choi, C.; Kim, M. S.; Lee, M.; Liu, S.; Cho, K. W.; Kim, H. M.; Cho, H.; Choi, M. K.; Lu, N.; Song, Y. M.; Kim, D.-H. An Aquatic-Vision-Inspired Camera Based on a Monocentric Lens and a Silicon Nanorod Photodiode Array. *Nat. Electron.* **2020**, *3*, 546−553.

(15) Thiele, S.; Arzenbacher, K.; Gissibl, T.; Giessen, H.; Herkommer, A. M. 3D-Printed Eagle Eye: Compound Microlens System for Foveated Imaging. *Sci. Adv.* **2017**, *3*, e1602655.

(16) Yoneda, K.; Suganuma, N.; Yanase, R.; Aldibaja, M. Automated Driving Recognition Technologies for Adverse Weather Conditions. *IATSS Research.* **2019**, *43*, 253−262.

(17) Kim, M.; Chang, S.; Kim, M.; Yeo, J. E.; Kim, M. S.; Lee, G. J.; Kim, D.-H.; Song, Y. M. Cuttlefish Eye-Inspired Artificial Vision for High-Quality Imaging under Uneven Illumination Conditions. *Sci. Robot.* **2023**, *8*, eade4698.

(18) Liao, F.; Zhou, Z.; Kim, B. J.; Chen, J.; Wang, J.; Wan, T.; Zhou, Y.; Hoang, A. T.; Wang, C.; Kang, J.; Ahn, J. H.; Chai, Y. Bioinspired In-Sensor Visual Adaptation for Accurate Perception. *Nat. Electron.* **2022**, *5*, 84−91.

(19) Mennel, L.; Symonowicz, J.; Wachter, S.; Polyushkin, D. K.; Molina-Mendoza, A. J.; Mueller, T. Ultrafast Machine Vision with 2D Material Neural Network Image Sensors. *Nature* **2020**, *579*, 62−66.

(20) Lee, M.; Seung, H.; Kwon, J. I.; Choi, M. K.; Kim, D.-H.; Choi, C. Nanomaterial-Based Synaptic Optoelectronic Devices for In-Sensor Preprocessing of Image Data. *ACS Omega* **2023**, *8*, 5209−5224.

(21) Lee, D.; Park, M.; Baek, Y.; Bae, B.; Heo, J.; Lee, K. In-Sensor Image Memorization and Encoding via Optical Neurons for Bio-Stimulus Domain Reduction toward Visual Cognitive Processing. *Nat. Commun.* **2022**, *13*, 5223.

(22) Dodda, A.; Jayachandran, D.; Pannone, A.; Trainor, N.; Stepanoff, S. P.; Steves, M. A.; Radhakrishnan, S. S.; Bachu, S.; Ordonez, C. W.; Shallenberger, J. R.; Redwing, J. M.; Knappenberger, K. L.; Wolfe, D. E.; Das, S. Active Pixel Sensor Matrix Based on Monolayer MoS_2 Phototransistor Array. *Nat. Mater.* **2022**, *21*, 1379−1387.

(23) Yeon, H.; Lin, P.; Choi, C.; Tan, S. H.; Park, Y.; Lee, D.; Lee, J.; Xu, F.; Gao, B.; Wu, H.; Qian, H.; Nie, Y.; Kim, S.; Kim, J. Alloying Conducting Channels for Reliable Neuromorphic Computing. *Nat. Nanotechnol.* **2020**, *15*, 574−579.

(24) Hu, Z. Y.; Zhang, Y. L.; Pan, C.; Dou, J. Y.; Li, Z. Z.; Tian, Z. N.; Mao, J. W.; Chen, Q. D.; Sun, H. B. Miniature Optoelectronic Compound Eye Camera. *Nat. Commun.* **2022**, *13*, 5634.

(25) Zhou, F.; Chai, Y. Near-Sensor and in-Sensor Computing. *Nat. Electron.* **2020**, *3*, 664−671.

(26) Kim, J. J.; Liu, H.; Ousati Ashtiani, A.; Jiang, H. Biologically Inspired Artificial Eyes and Photonics. *Rep. Prog. Phys.* **2020**, *83*, 047101.

(27) Lee, G. J.; Choi, C.; Kim, D.-H.; Song, Y. M. Bioinspired Artificial Eyes: Optic Components, Digital Cameras, and Visual Prostheses. *Adv. Funct. Mater.* **2018**, *28*, 1705202.

(28) Park, J.; Seung, H.; Kim, D. C.; Kim, M. S.; Kim, D.-H. Unconventional Image-Sensing and Light-Emitting Devices for Extended Reality. *Adv. Funct. Mater.* **2021**, *31*, 2009281.

(29) Lee, H.; Hwang, J. H.; Song, S. H.; Han, H.; Han, S. J.; Suh, B. L.; Hur, K.; Kyhm, J.; Ahn, J.; Cho, J. H.; Hwang, D. K.; Lee, E.; Choi, C.; Lim, J. A. Chiroptical Synaptic Heterojunction Phototransistors Based on Self-Assembled Nanohelix of π-Conjugated Molecules for Direct Noise-Reduced Detection of Circularly Polarized Light. *Adv. Sci.* **2023**, *10*, 2304039.

(30) Pi, L.; Wang, P.; Liang, S. J.; Luo, P.; Wang, H.; Li, D.; Li, Z.; Chen, P.; Zhou, X.; Miao, F.; Zhai, T. Broadband Convolutional Processing Using Band-Alignment-Tunable Heterostructures. *Nat. Electron.* **2022**, *5*, 248−254.

(31) Choi, C.; Leem, J.; Kim, M. S.; Taqieddin, A.; Cho, C.; Cho, K. W.; Lee, G. J.; Seung, H.; Bae, H. J.; Song, Y. M.; Hyeon, T.; Aluru, N. R.; Nam, S. W.; Kim, D.-H. Curved Neuromorphic Image Sensor Array Using a MoS_2-Organic Heterostructure Inspired by the Human Visual Recognition System. *Nat. Commun.* **2020**, *11*, 5934.

(32) Kim, M. S.; Yeo, J. E.; Choi, H.; Chang, S.; Kim, D.-H.; Song, Y. M. Evolution of Natural Eyes and Biomimetic Imaging Devices for Effective Image Acquisition. *J. Mater. Chem. C* **2023**, *11*, 12083−12104.

(33) Choi, C.; Choi, M. K.; Liu, S.; Kim, M. S.; Park, O. K.; Im, C.; Kim, J.; Qin, X.; Lee, G. J.; Cho, K. W.; Kim, M.; Joh, E.; Lee, J.; Son, D.; Kwon, S. H.; Jeon, N. L.; Song, Y. M.; Lu, N.; Kim, D.-H. Human Eye-Inspired Soft Optoelectronic Device Using High-Density MoS_2-Graphene Curved Image Sensor Array. *Nat. Commun.* **2017**, *8*, 1664.

(34) Zhang, K.; Jung, Y. H.; Mikael, S.; Seo, J. H.; Kim, M.; Mi, H.; Zhou, H.; Xia, Z.; Zhou, W.; Gong, S.; Ma, Z. Origami Silicon Optoelectronics for Hemispherical Electronic Eye Systems. *Nat. Commun.* **2017**, *8*, 1782.

(35) Ko, H. C.; Stoykovich, M. P.; Song, J.; Malyarchuk, V.; Choi, W. M.; Yu, C. J.; Geddes, J. B.; Xiao, J.; Wang, S.; Huang, Y.; Rogers, J. A. A Hemispherical Electronic Eye Camera Based on Compressible Silicon Optoelectronics. *Nature* **2008**, *454*, 748−753.

(36) Hu, Y.; Dai, M.; Feng, W.; Zhang, X.; Gao, F.; Zhang, S.; Tan, B.; Zhang, J.; Shuai, Y.; Fu, Y. Q.; Hu, P. A. Ultralow Power Optical

https://doi.org/10.1021/acsnano.3c10181
ACS Nano XXXX, XXX, XXX−XXX

Synapses Based on MoS_2 Layers by Indium-Induced Surface Charge Doping for Biomimetic Eyes. *Adv. Mater.* **2021**, *33*, 2104960.
(37) Lee, K.; Han, H.; Kim, Y.; Park, J.; Jang, S.; Lee, H.; Lee, S. W.; Kim, H. Y.; Kim, Y.; Kim, T.; Kim, D.; Wang, G.; Park, C. Retina-Inspired Structurally Tunable Synaptic Perovskite Nanocones. *Adv. Funct. Mater.* **2021**, *31*, 2105596.
(38) Hong, S.; Cho, H.; Kang, B. H.; Park, K.; Akinwande, D.; Kim, H. J.; Kim, S. Neuromorphic Active Pixel Image Sensor Array for Visual Memory. *ACS Nano* **2021**, *15*, 15362−15370.
(39) Rao, Z.; Lu, Y.; Li, Z.; Sim, K.; Ma, Z.; Xiao, J.; Yu, C. Curvy, Shape-Adaptive Imagers Based on Printed Optoelectronic Pixels with a Kirigami Design. *Nat. Electron.* **2021**, *4*, 513−521.
(40) Jung, I.; Xiao, J.; Malyarchuk, V.; Lu, C.; Li, M.; Liu, Z.; Yoon, J.; Huang, Y.; Rogers, J. A. Dynamically Tunable Hemispherical Electronic Eye Camera System with Adjustable Zoom Capability. *Proc. Natl. Acad. Sci. U.S.A.* **2011**, *108*, 1788−1793.
(41) Akinwande, D.; Petrone, N.; Hone, J. Two-Dimensional Flexible Nanoelectronics. *Nat. Commun.* **2014**, *5*, 5678.
(42) Manzeli, S.; Ovchinnikov, D.; Pasquier, D.; Yazyev, O. V.; Kis, A. 2D Transition Metal Dichalcogenides. *Nat. Rev. Mater.* **2017**, *2*, 17033.
(43) Lee, W.; Liu, Y.; Lee, Y.; Sharma, B. K.; Shinde, S. M.; Kim, S. D.; Nan, K.; Yan, Z.; Han, M.; Huang, Y.; Zhang, Y.; Ahn, J. H.; Rogers, J. A. Two-Dimensional Materials in Functional Three-Dimensional Architectures with Applications in Photodetection and Imaging. *Nat. Commun.* **2018**, *9*, 1417.
(44) Zhang, Y.; Wang, L.; Lei, Y.; Wang, B.; Lu, Y.; Yao, Y.; Zhang, N.; Lin, D.; Jiang, Z.; Guo, H.; Zhang, J.; Hu, H. Self-Powered Bidirectional Photoresponse in High-Detectivity WSe_2 Phototransistor with Asymmetrical van Der Waals Stacking for Retinal Neurons Emulation. *ACS Nano* **2022**, *16*, 20937−20945.
(45) Lee, M.; Lee, W.; Choi, S.; Jo, J. W.; Kim, J.; Park, S. K.; Kim, Y. H. Brain-Inspired Photonic Neuromorphic Devices Using Photodynamic Amorphous Oxide Semiconductors and Their Persistent Photoconductivity. *Adv. Mater.* **2017**, *29*, 1700951.
(46) Wang, X.; Chen, C.; Zhu, L.; Shi, K.; Peng, B.; Zhu, Y.; Mao, H.; Long, H.; Ke, S.; Fu, C.; Zhu, Y.; Wan, C.; Wan, Q. Vertically Integrated Spiking Cone Photoreceptor Arrays for Color Perception. *Nat. Commun.* **2023**, *14*, 3444.
(47) Song, J. K.; Kim, J.; Yoon, J.; Koo, J. H.; Jung, H.; Kang, K.; Sunwoo, S. H.; Yoo, S.; Chang, H.; Jo, J.; Baek, W.; Lee, S.; Lee, M.; Kim, H. J.; Shin, M.; Yoo, Y. J.; Song, Y. M.; Hyeon, T.; Kim, D.-H.; Son, D. Stretchable Colour-Sensitive Quantum Dot Nanocomposites for Shape-Tunable Multiplexed Phototransistor Arrays. *Nat. Nanotechnol.* **2022**, *17*, 849−856.
(48) Jo, C.; Kim, J.; Kwak, J. Y.; Kwon, S. M.; Park, J. B.; Kim, J.; Park, G. S.; Kim, M. G.; Kim, Y. H.; Park, S. K. Retina-Inspired Color-Cognitive Learning via Chromatically Controllable Mixed Quantum Dot Synaptic Transistor Arrays. *Adv. Mater.* **2022**, *34*, 2108979.
(49) Lee, W.; Lee, J.; Yun, H.; Kim, J.; Park, J.; Choi, C.; Kim, D. C.; Seo, H.; Lee, H.; Yu, J. W.; Lee, W. B.; Kim, D.-H. High-Resolution Spin-on-Patterning of Perovskite Thin Films for a Multiplexed Image Sensor Array. *Adv. Mater.* **2017**, *29*, 1702902.
(50) Zhang, M. N.; Wu, X.; Riaud, A.; Wang, X. L.; Xie, F.; Liu, W. J.; Mei, Y.; Zhang, D. W.; Ding, S. J. Spectrum Projection with a Bandgap-Gradient Perovskite Cell for Colour Perception. *Light Sci. Appl.* **2020**, *9*, 162.
(51) Liu, Y.; Ji, Z.; Cen, G.; Sun, H.; Wang, H.; Zhao, C.; Wang, Z. L.; Mai, W. Perovskite-Based Color Camera Inspired by Human Visual Cells. *Light Sci. Appl.* **2023**, *12*, 43.
(52) Sim, K.; Chen, S.; Li, Z.; Rao, Z.; Liu, J.; Lu, Y.; Jang, S.; Ershad, F.; Chen, J.; Xiao, J.; Yu, C. Three-Dimensional Curvy Electronics Created Using Conformal Additive Stamp Printing. *Nat. Electron.* **2019**, *2*, 471−479.
(53) Shin, G.; Jung, I.; Malyarchuk, V.; Song, J.; Wang, S.; Ko, H. C.; Huang, Y.; Ha, J. S.; Rogers, J. A. Micromechanics and Advanced Designs for Curved Photodetector Arrays in Hemispherical Electronic-Eye Cameras. *Small* **2010**, *6*, 851−856.
(54) Song, Y. M.; Xie, Y.; Malyarchuk, V.; Xiao, J.; Jung, I.; Choi, K. J.; Liu, Z.; Park, H.; Lu, C.; Kim, R. H.; Li, R.; Crozier, K. B.; Huang, Y.; Rogers, J. A. Digital Cameras with Designs Inspired by the Arthropod Eye. *Nature* **2013**, *497*, 95−99.
(55) Shim, H.; Ershad, F.; Patel, S.; Zhang, Y.; Wang, B.; Chen, Z.; Marks, T. J.; Facchetti, A.; Yu, C. An Elastic and Reconfigurable Synaptic Transistor Based on a Stretchable Bilayer Semiconductor. *Nat. Electron.* **2022**, *5*, 660−671.
(56) Kim, J.; Lee, M.; Shim, H. J.; Ghaffari, R.; Cho, H. R.; Son, D.; Jung, Y. H.; Soh, M.; Choi, C.; Jung, S.; Chu, K.; Jeon, D.; Lee, S. T.; Kim, J. H.; Choi, S. H.; Hyeon, T.; Kim, D.-H. Stretchable Silicon Nanoribbon Electronics for Skin Prosthesis. *Nat. Commun.* **2014**, *5*, 5747.
(57) Seo, S.; Jo, S. H.; Kim, S.; Shim, J.; Oh, S.; Kim, J. H.; Heo, K.; Choi, J. W.; Choi, C.; Oh, S.; Kuzum, D.; Wong, H. S. P.; Park, J. H. Artificial Optic-Neural Synapse for Colored and Color-Mixed Pattern Recognition. *Nat. Commun.* **2018**, *9*, 5106.
(58) Lee, S.; Peng, R.; Wu, C.; Li, M. Programmable Black Phosphorus Image Sensor for Broadband Optoelectronic Edge Computing. *Nat. Commun.* **2022**, *13*, 1485.
(59) Choi, C.; Lee, Y.; Cho, K. W.; Koo, J. H.; Kim, D.-H. Wearable and Implantable Soft Bioelectronics Using Two-Dimensional Materials. *Acc. Chem. Res.* **2019**, *52*, 73−81.
(60) Song, S.; Choi, C.; Ahn, J.; Lee, J. J.; Jang, J.; Yu, B. S.; Hong, J. P.; Ryu, Y. S.; Kim, Y. H.; Hwang, D. K. Artificial Optoelectronic Synapse Based on Spatiotemporal Irradiation to Source-Sharing Circuitry of Synaptic Phototransistors. *InfoMat* **2023**, DOI: 10.1002/inf2.12479.
(61) Kumar, M.; Lim, J.; Kim, S.; Seo, H. Environment-Adaptable Photonic-Electronic-Coupled Neuromorphic Angular Visual System. *ACS Nano* **2020**, *14*, 14108−14117.
(62) Kwon, S. M.; Kwak, J. Y.; Song, S.; Kim, J.; Jo, C.; Cho, S. S.; Nam, S. J.; Kim, J.; Park, G. S.; Kim, Y. H.; Park, S. K. Large-Area Pixelized Optoelectronic Neuromorphic Devices with Multispectral Light-Modulated Bidirectional Synaptic Circuits. *Adv. Mater.* **2021**, *33*, 2105017.
(63) Li, S.; Jang, J. H.; Chung, W.; Seung, H.; Park, S. I.; Ma, H.; Pyo, W. J.; Choi, C.; Chung, D. S.; Kim, D.-H.; Choi, M. K.; Yang, J. Ultrathin Self-Powered Heavy-Metal-Free Cu-In-Se Quantum Dot Photodetectors for Wearable Health Monitoring. *ACS Nano* **2023**, *17*, 20013−20023.
(64) Vijjapu, M. T.; Fouda, M. E.; Agambayev, A.; Kang, C. H.; Lin, C. H.; Ooi, B. S.; He, J. H.; Eltawil, A. M.; Salama, K. N. A Flexible Capacitive Photoreceptor for the Biomimetic Retina. *Light Sci. Appl.* **2022**, *11*, 3.
(65) Tsai, W. L.; Chen, C. Y.; Wen, Y. T.; Yang, L.; Cheng, Y. L.; Lin, H. W. Band Tunable Microcavity Perovskite Artificial Human Photoreceptors. *Adv. Mater.* **2019**, *31*, 1900231.
(66) Chen, S.; Huang, J. Recent Advances in Synaptic Devices Based on Halide Perovskite. *ACS Appl. Electron. Mater.* **2020**, *2*, 1815−1825.
(67) Shao, H.; Li, Y.; Yang, W.; He, X.; Wang, L.; Fu, J.; Fu, M.; Ling, H.; Gkoupidenis, P.; Yan, F.; Xie, L.; Huang, W. A Reconfigurable Optoelectronic Synaptic Transistor with Stable Zr-CsPbI3 Nanocrystals for Visuomorphic Computing. *Adv. Mater.* **2023**, *35*, 2208497.
(68) He, Z.; Shen, H.; Ye, D.; Xiang, L.; Zhao, W.; Ding, J.; Zhang, F.; Di, C. an; Zhu, D. An Organic Transistor with Light Intensity-Dependent Active Photoadaptation. *Nat. Electron.* **2021**, *4*, 522−529.
(69) Kim, Y.; Zhu, C.; Lee, W. Y.; Smith, A.; Ma, H.; Li, X.; Son, D.; Matsuhisa, N.; Kim, J.; Bae, W. G.; Cho, S. H.; Kim, M. G.; Kurosawa, T.; Katsumata, T.; To, J. W. F.; Oh, J. Y.; Paik, S.; Kim, S. J.; Jin, L.; Yan, F.; Tok, J. B. H.; Bao, Z. A Hemispherical Image Sensor Array Fabricated with Organic Photomemory Transistors. *Adv. Mater.* **2023**, *35*, 2203541.
(70) Chen, K.; Hu, H.; Song, I.; Gobeze, H. B.; Lee, W. J.; Abtahi, A.; Schanze, K. S.; Mei, J. Organic Optoelectronic Synapse Based on Photon-Modulated Electrochemical Doping. *Nat. Photonics* **2023**, *17*, 629−637.

https://doi.org/10.1021/acsnano.3c10181
ACS Nano XXXX, XXX, XXX−XXX

(71) Shim, H. J.; Sunwoo, S. H.; Kim, Y.; Koo, J. H.; Kim, D.-H. Functionalized Elastomers for Intrinsically Soft and Biointegrated Electronics. *Adv. Healthc. Mater.* **2021**, *10*, 2002105.
(72) Gu, L.; Poddar, S.; Lin, Y.; Long, Z.; Zhang, D.; Zhang, Q.; Shu, L.; Qiu, X.; Kam, M.; Javey, A.; Fan, Z. A Biomimetic Eye with a Hemispherical Perovskite Nanowire Array Retina. *Nature* **2020**, *581*, 278−282.
(73) Chen, C.; He, Y.; Mao, H.; Zhu, L.; Wang, X.; Zhu, Y.; Zhu, Y.; Shi, Y.; Wan, C.; Wan, Q. A Photoelectric Spiking Neuron for Visual Depth Perception. *Adv. Mater.* **2022**, *34*, 2201895.
(74) Currea, J. P.; Sondhi, Y.; Kawahara, A. Y.; Theobald, J. Measuring Compound Eye Optics with Microscope and MicroCT Images. *Commun. Biol.* **2023**, *6*, 246.
(75) Ma, Z. C.; Hu, X. Y.; Zhang, Y. L.; Liu, X. Q.; Hou, Z. S.; Niu, L. G.; Zhu, L.; Han, B.; Chen, Q. D.; Sun, H. B. Smart Compound Eyes Enable Tunable Imaging. *Adv. Funct. Mater.* **2019**, *29*, 1903340.
(76) Floreano, D.; Pericet-Camara, R.; Viollet, S.; Ruffier, F.; Brückner, A.; Leitel, R.; Buss, W.; Menouni, M.; Expert, F.; Juston, R.; Dobrzynski, M. K.; L'Eplattenier, G.; Recktenwald, F.; Mallot, H. A.; Franceschini, N. Miniature Curved Artificial Compound Eyes. *Proc. Natl. Acad. Sci. U.S.A.* **2013**, *110*, 9267−9272.
(77) Lee, M.; Lee, G. J.; Jang, H. J.; Joh, E.; Cho, H.; Kim, M. S.; Kim, H. M.; Kang, K. M.; Lee, J. H.; Kim, M.; Jang, H.; Yeo, J. E.; Durand, F.; Lu, N.; Kim, D.-H.; Song, Y. M. An Amphibious Artificial Vision System with a Panoramic Visual Field. *Nat. Electron.* **2022**, *5*, 452−459.
(78) Alkaladi, A.; Zeil, J. Functional Anatomy of the Fiddler Crab Compound Eye (Uca Vomeris: Ocypodidae, Brachyura, Decapoda). *J. Comp. Neurol.* **2014**, *522*, 1264−1283.
(79) Wang, Y.; Cai, Y.; Wang, F.; Yang, J.; Yan, T.; Li, S.; Wu, Z.; Zhan, X.; Xu, K.; He, J.; Wang, Z. A Three-Dimensional Neuromorphic Photosensor Array for Nonvolatile In-Sensor Computing. *Nano Lett.* **2023**, *23*, 4524−4532.
(80) Jayachandran, D.; Pannone, A.; Das, M.; Schranghamer, T. F.; Sen, D.; Das, S. Insect-Inspired, Spike-Based, in-Sensor, and Night-Time Collision Detector Based on Atomically Thin and Light-Sensitive Memtransistors. *ACS Nano* **2023**, *17*, 1068−1080.
(81) Zhou, F.; Zhou, Z.; Chen, J.; Choy, T. H.; Wang, J.; Zhang, N.; Lin, Z.; Yu, S.; Kang, J.; Wong, H. S. P.; Chai, Y. Optoelectronic Resistive Random Access Memory for Neuromorphic Vision Sensors. *Nat. Nanotechnol.* **2019**, *14*, 776−782.
(82) Cai, Y.; Wang, F.; Wang, X.; Li, S.; Wang, Y.; Yang, J.; Yan, T.; Zhan, X.; Wang, F.; Cheng, R.; He, J.; Wang, Z. Broadband Visual Adaption and Image Recognition in a Monolithic Neuromorphic Machine Vision System. *Adv. Funct. Mater.* **2023**, *33*, 2212917.
(83) Shan, X.; Zhao, C.; Wang, X.; Wang, Z.; Fu, S.; Lin, Y.; Zeng, T.; Zhao, X.; Xu, H.; Zhang, X.; Liu, Y. Plasmonic Optoelectronic Memristor Enabling Fully Light-Modulated Synaptic Plasticity for Neuromorphic Vision. *Adv. Sci.* **2022**, *9*, 2104632.
(84) Radhakrishnan, S. S.; Sebastian, A.; Oberoi, A.; Das, S.; Das, S. A Biomimetic Neural Encoder for Spiking Neural Network. *Nat. Commun.* **2021**, *12*, 2143.
(85) Seung, H.; Choi, C.; Kim, D. C.; Kim, J. S.; Kim, J. H.; Kim, J.; Park, S. I.; Lim, J. A.; Yang, J.; Choi, M. K.; Hyeon, T.; Kim, D.-H. Integration of Synaptic Phototransistors and Quantum Dot Light-Emitting Diodes for Visualization and Recognition of UV Patterns. *Sci. Adv.* **2022**, *8*, eabq3101.
(86) Hong, S.; Choi, S. H.; Park, J.; Yoo, H.; Oh, J. Y.; Hwang, E.; Yoon, D. H.; Kim, S. Sensory Adaptation and Neuromorphic Phototransistors Based on $CsPb(Br_{1-X}I_x)_3$ Perovskite and MoS_2 Hybrid Structure. *ACS Nano* **2020**, *14*, 9796−9806.
(87) Han, M. J.; Tsukruk, V. V. Trainable Bilingual Synaptic Functions in Bio-Enabled Synaptic Transistors. *ACS Nano* **2023**, *17*, 18883−18892.
(88) Chen, J.; Zhou, Z.; Kim, B. J.; Zhou, Y.; Wang, Z.; Wan, T.; Yan, J.; Kang, J.; Ahn, J. H.; Chai, Y. Optoelectronic Graded Neurons for Bioinspired In-Sensor Motion Perception. *Nat. Nanotechnol.* **2023**, *18*, 882−888.
(89) Choi, C.; Kim, H.; Kang, J. H.; Song, M. K.; Yeon, H.; Chang, C. S.; Suh, J. M.; Shin, J.; Lu, K.; Park, B. I.; Kim, Y.; Lee, H. E.; Lee, D.; Lee, J.; Jang, I.; Pang, S.; Ryu, K.; Bae, S. H.; Nie, Y.; Kum, H. S.; Park, M. C.; Lee, S.; Kim, H. J.; Wu, H.; Lin, P.; Kim, J. Reconfigurable Heterogeneous Integration Using Stackable Chips with Embedded Artificial Intelligence. *Nat. Electron.* **2022**, *5*, 386−393.
(90) Cho, H.; Lee, I.; Jang, J.; Kim, J. H.; Lee, H.; Park, S.; Wang, G. Real-Time Finger Motion Recognition Using Skin-Conformable Electronics. *Nat. Electron.* **2023**, *6* (8), 619−629.
(91) Jang, H.; Hinton, H.; Jung, W. B.; Lee, M. H.; Kim, C.; Park, M.; Lee, S. K.; Park, S.; Ham, D. In-Sensor Optoelectronic Computing Using Electrostatically Doped Silicon. *Nat. Electron.* **2022**, *5*, 519−525.
(92) Banks, M. S.; Sprague, W. W.; Schmoll, J.; Parnell, J. A. Q.; Love, G. D. Why Do Animal Eyes Have Pupils of Different Shapes? *Sci. Adv.* **2015**, *1*, e1500391.
(93) López-Gil, N.; Fernández-Sánchez, V. The Change of Spherical Aberration during Accommodation and Its Effect on the Accommodation Response. *J. Vis.* **2010**, *10*, 10−12.
(94) Bringmann, A. Structure and Function of the Bird Fovea. *Anat. Histol. Embryol.* **2019**, *48*, 177−200.
(95) Keum, D.; Jung, H.; Jeong, K. H. Planar Emulation of Natural Compound Eyes. *Small* **2012**, *8*, 2169−2173.
(96) Dai, B.; Zhang, L.; Zhao, C.; Bachman, H.; Becker, R.; Mai, J.; Jiao, Z.; Li, W.; Zheng, L.; Wan, X.; Huang, T. J.; Zhuang, S.; Zhang, D. Biomimetic Apposition Compound Eye Fabricated Using Microfluidic-Assisted 3D Printing. *Nat. Commun.* **2021**, *12*, 6458.
(97) Petsch, S.; Schuhladen, S.; Dreesen, L.; Zappe, H. The Engineered Eyeball, a Tunable Imaging System Using Soft-Matter Micro-Optics. *Light Sci. Appl.* **2016**, *5*, e16068.
(98) Hartmann, F.; Penkner, L.; Danninger, D.; Arnold, N.; Kaltenbrunner, M. Soft Tunable Lenses Based on Zipping Electroactive Polymer Actuators. *Adv. Sci.* **2021**, *8*, 2003104.
(99) Li, J.; Wang, Y.; Liu, L.; Xu, S.; Liu, Y.; Leng, J.; Cai, S. A Biomimetic Soft Lens Controlled by Electrooculographic Signal. *Adv. Funct. Mater.* **2019**, *29*, 103762.
(100) Park, J.; Lee, Y.; Lee, H.; Ko, H. Transfer Printing of Electronic Functions on Arbitrary Complex Surfaces. *ACS Nano* **2020**, *14*, 12−20.
(101) Song, J. K.; Kim, M. S.; Yoo, S.; Koo, J. H.; Kim, D. H. Materials and Devices for Flexible and Stretchable Photodetectors and Light-Emitting Diodes. *Nano Res.* **2021**, *14*, 2919−2937.
(102) Jiang, T.; Wang, Y.; Zheng, Y.; Wang, L.; He, X.; Li, L.; Deng, Y.; Dong, H.; Tian, H.; Geng, Y.; Xie, L.; Lei, Y.; Ling, H.; Ji, D.; Hu, W. Tetrachromatic Vision-Inspired Neuromorphic Sensors with Ultraweak Ultraviolet Detection. *Nat. Commun.* **2023**, *14*, 2281.
(103) Kim, M. S.; Kim, M. S.; Lee, G. J.; Sunwoo, S. H.; Chang, S.; Song, Y. M.; Kim, D.-H. Bio-Inspired Artificial Vision and Neuromorphic Image Processing Devices. *Adv. Mater. Technol.* **2022**, *7*, 2100144.
(104) Zhu, Q. B.; Li, B.; Yang, D. D.; Liu, C.; Feng, S.; Chen, M. L.; Sun, Y.; Tian, Y. N.; Su, X.; Wang, X. M.; Qiu, S.; Li, Q. W.; Li, X. M.; Zeng, H. B.; Cheng, H. M.; Sun, D. M. A Flexible Ultrasensitive Optoelectronic Sensor Array for Neuromorphic Vision Systems. *Nat. Commun.* **2021**, *12*, 1798.
(105) Abbott, J.; Ye, T.; Krenek, K.; Gertner, R. S.; Ban, S.; Kim, Y.; Qin, L.; Wu, W.; Park, H.; Ham, D. A Nanoelectrode Array for Obtaining Intracellular Recordings from Thousands of Connected Neurons. *Nat. Biomed. Eng.* **2020**, *4*, 232−241.
(106) Dodda, A.; Jayachandran, D.; Subbulakshmi Radhakrishnan, S.; Pannone, A.; Zhang, Y.; Trainor, N.; Redwing, J. M.; Das, S. Bioinspired and Low-Power 2D Machine Vision with Adaptive Machine Learning and Forgetting. *ACS Nano* **2022**, *16*, 20010−20020.
(107) Kim, J.; Lee, H. C.; Kim, K. H.; Hwang, M. S.; Park, J. S.; Lee, J. M.; So, J. P.; Choi, J. H.; Kwon, S. H.; Barrelet, C. J.; Park, H. G. Photon-Triggered Nanowire Transistors. *Nat. Nanotechnol.* **2017**, *12*, 963−968.

https://doi.org/10.1021/acsnano.3c10181
ACS Nano XXXX, XXX, XXX−XXX

(108) Hou, Y. X.; Li, Y.; Zhang, Z. C.; Li, J. Q.; Qi, D. H.; Chen, X. D.; Wang, J. J.; Yao, B. W.; Yu, M. X.; Lu, T. B.; Zhang, J. Large-Scale and Flexible Optical Synapses for Neuromorphic Computing and Integrated Visible Information Sensing Memory Processing. *ACS Nano* **2021**, *15*, 1497−1508.
(109) Koo, J. H.; Kang, J.; Lee, S.; Song, J. K.; Choi, J.; Yoon, J.; Park, H. J.; Sunwoo, S. H.; Kim, D. C.; Nam, W.; Kim, D.-H.; Im, S. G.; Son, D. A Vacuum-Deposited Polymer Dielectric for Wafer-Scale Stretchable Electronics. *Nat. Electron* **2023**, *6*, 137−145.
(110) Yuan, S.; Ma, C.; Fetaya, E.; Mueller, T.; Naveh, D.; Zhang, F.; Xia, F. Geometric Deep Optical Sensing. *Science* **2023**, *379*, eade1220.

https://doi.org/10.1021/acsnano.3c10181
ACS Nano XXXX, XXX, XXX−XXX